Innate immune pathways act synergistically to constrain RNA virus evolution in Drosophila melanogaster

Vanesa Mongelli, Sebastian Lequime, Athanasios Kousathanas, Valérie Gausson, Hervé Blanc, Jared Nigg, Lluis Quintana-Murci, Santiago Elena, Maria-Carla P Saleh

Innate immune pathways act synergistically to constrain RNA virus evolution in *Drosophila melanogaster*

Vanesa Mongelli[1], Sebastian Lequime[2], Athanasios Kousathanas[3], Valérie Gausson[1], Hervé Blanc[1], Jared Nigg[1], Lluis Quintana-Murci[3,4], Santiago F. Elena[5,6]*, Maria-Carla Saleh[1]*

[1] Viruses and RNA Interference Unit, Institut Pasteur, UMR3569, CNRS, Paris, France.

[2] Cluster of Microbial Ecology, Groningen Institute for Evolutionary Life Sciences, University of Groningen, Groningen, The Netherlands.

[3] Human Evolutionary Genetic Unit, Institut Pasteur, UMR2000, CNRS, Paris, France.

[4] Human Genomics and Evolution, Collège de France, Paris, France.

[5] Instituto de Biología Integrativa de Sistemas (CSIC – Universitat de València), Paterna, 46182 València, Spain.

[6] The Santa Fe Institute, Santa Fe NM87501, USA.

*email: santiago.elena@csic.es; carla.saleh@pasteur.fr

Abstract

Host-pathogen interactions impose recurrent selective pressures that lead to constant adaptation and counter-adaptation in both competing species. Here, we sought to study this evolutionary arms-race and assessed the impact of the innate immune system on viral population diversity and evolution, using *Drosophila melanogaster* as model host and its natural pathogen Drosophila C virus (DCV). We isogenized eight fly genotypes generating animals defective for RNAi, Imd and Toll innate immune pathways as well as pathogen sensing and gut renewal pathways. Wild-type or mutant flies were then orally infected with DCV, and the virus was serially passaged ten times via reinfection in naïve flies. Viral population diversity was studied after each viral passage by high-throughput sequencing, and infection phenotypes were assessed at the beginning and at the end of the evolution experiment. We found that the absence of any of the various immune pathways studied increased viral genetic diversity while attenuating virulence. Strikingly, these effects were observed in a range of host factors described as having mainly antiviral or antibacterial functions. Together, our results indicate that the innate immune system as a whole, and not specific antiviral defense pathways in isolation, generally constrains viral diversity and evolution.

Introduction

Interaction between hosts and pathogens trigger defense and counter-defense mechanisms that often result in reciprocal adaptation and coevolution of both organisms[1]. Empirical evidence of such arms-races involving both species can be drawn from genome-wide analysis of hosts and pathogens and in experimental evolution settings. For example, evolutionary analysis of mammalian genomes has revealed evidence of host-virus coevolution between different retroviruses and antiviral factors[2,3], and in plants, host resistance genes and virulence genes encoded by pathogens have been found to co-evolve[4]. Likewise, between bacteria and their infecting bacteriophages, experimental co-evolution studies resulted in the occurrence of genetic variants in both a bacterial lipopolysaccharide synthesis gene and the phage tail fiber gene which binds to lipopolysaccharide during adsorption[5]. In nematodes and their pathogenic bacteria, the number of toxin-expressing plasmids varies during adaptation to the host[6].

In insects, analyses of sequences within and between Drosophila species have shown evidence of adaptive evolution in immunity related genes[7–10]. In a study that deep sequenced siRNAs from mosquitoes infected with West Nile virus, it was found that the regions of the viral genome more intensively targeted by RNA interference (RNAi) contained a higher number of mutations than genomic regions less affected by this pathway, suggesting that this antiviral defense mechanism imposes a selective pressure on the viral population[11]. Similar observations on the selective pressure imposed by the RNAi pathway on viral evolution have been made in plant- and human-infecting viruses[12–16]. *Drosophila melanogaster* is a well-studied insect model to decipher virus-host interactions and therefore the impact of host antiviral

immunity on viral diversity and evolution. Different Drosophila immune pathways and mechanisms are involved in antiviral defense[17,18]. As is the case for all invertebrates, defense against pathogens in Drosophila relies on innate immunity, which constitutes the first and only defense against microbes. Innate immunity is characterized by the recognition of pathogen derived molecules, called pathogen-associated molecular patterns (PAMPs), by host encoded receptors (pathogen recognition receptors – PRRs), which leads to a rapid defense response.

The RNAi mechanism is known to play a central role in Drosophila antiviral defense, mainly through the action of the small interfering (si) RNA pathway[19–22]. Antiviral RNAi is triggered by virtually all insect-infecting viruses, resulting in targeting of the viral genome in a sequence-specific manner to control infection. Several other pathways have antiviral properties in flies, but their roles against viruses seem to be virus specific. The Toll and Imd (Immune deficiency) pathways, originally described to be involved in antibacterial and antifungal responses, have been shown to play a role in antiviral defense against Drosophila C virus (DCV), Cricket paralysis virus (CrPV), Drosophila X virus, Nora virus, and Flock house virus[23–26]. The Janus kinase signal transducers and activators of transcription (JAK-STAT) pathway can be activated upon DCV or CrPV infection in flies, triggering the expression of antiviral factors[27,28].

DCV, a positive-sense single stranded RNA virus from the genus *Cripavirus* within the *Dicistrioviridae* family and *Picornavirales* order[29], is a well characterized natural pathogen of the fruit fly that can be found in laboratory and wild populations[30]. As for many other Drosophila-infecting viruses, defense against DCV depends on the joint action of different innate immune pathways and mechanisms. RNAi, Toll and

86 Imd pathways, but also the protein encoded by the gene *Vago*, play a role in the
87 defense against this virus[20,24–27,31–33]. DCV is thought to be naturally acquired by
88 ingestion[30,34,35]. For orally acquired pathogens, the digestive tract, and the gut in
89 particular, represents the first host defense barrier. Despite many studies using oral
90 bacterial infections[36], the role of gut-specific antiviral responses in Drosophila is not
91 fully understood. Responses triggered against bacterial pathogens in the gut include
92 the production of reactive oxygen species and antimicrobial peptides, as well as
93 tissue repair and regeneration mechanisms[37]. Furthermore, the maintenance of gut
94 homeostasis after tissue damage caused by pathogenic bacteria relies on the activity
95 of JAK-STAT and epidermal growth factor receptor (EGFR) pathways, amongst
96 others[37–39]. In the hallmark of viral infections, a role of the Imd and extracellular-
97 signal-regulated kinase (ERK) pathways in the antiviral response in the gut has been
98 suggested[24,40]. It is important to note that, like many other RNA viruses with error-
99 prone polymerases and fast replication kinetics, DCV exists as large populations
100 composed of a cloud of genetically related mutant variants known as viral
101 quasispecies or mutant swarms[41]. Viral mutant swarms constitute a dynamic
102 repertoire of genetic and phenotypic variability that renders great adaptability.
103 In this work, we leveraged the vast knowledge on antiviral mechanisms, the
104 extensive genetic tool-box available for *D. melanogaster*, the intrinsic variability of the
105 DCV mutant swarms, and the great depth power of next generation sequencing to
106 study the impact of innate immune pathways on viral diversity and evolution. We
107 aimed to determine not only if each pathway has a specific impact on the selective
108 pressure imposed to DCV mutant swarms, but also their relative impact. In addition,
109 we investigated possible links between selected viral variants (viral function) and

specific defense mechanisms. Our results with infections in flies defective for several immune pathways show that the host genotype has an impact on viral genetic diversity regardless of the immune pathway being affected and this is accompanied by an attenuation of the virulence along evolutionary passages. We also describe complex mutation dynamics, with several examples of clonal interference in which increases in frequency of adaptive mutations have been displaced by other mutations of stronger effect that arose in different genetic backgrounds. Overall, our results highlight that innate immune pathways constrain RNA virus evolution and further demonstrate that antiviral responses in Drosophila are likely polygenic.

Results

Production of fly mutant lines for innate immune pathways

To determine the impact of the innate immune system on virus population diversity and evolution, we selected fly lines with impaired function in genes belonging to most of the Drosophila innate immune pathways: RNAi, Toll and Imd. We selected genes encoding for proteins involved both upstream and downstream of the immune pathways, such as receptors or ligands that trigger the immune response, and effectors of the response (Figure 1a). For the RNAi pathway, Dicer 2 (Dcr-2) and Argonaute 2 (Ago-2); for the Toll pathway, the ligand of Toll receptor Spätzle (spz), and the NF-κB transcription factor Dorsal-related immunity factor (Dif); for the Imd pathway, the NF-κB transcription factor Relish (*Rel*). We also added to the study the host factor Vago, that is upregulated during viral infections in a Dicer 2-dependent manner. Because DCV is orally acquired, and to explore the impact of gut homeostasis on the antiviral response, a mutant line for Epidermal growth factor

receptor (*Egfr*), a gene involved in gut epithelium renewal, was also included in our panel. With the exception of *Egfr* and *Dif*, all of the selected genes were previously described to play an antiviral role against DCV infection[19–21,23–25]. It is important to mention that, in contrast to the RNAi antiviral mechanism that relies on the direct interaction between the components of the RNAi pathway and the viral genome, the molecular mechanisms underlying the antiviral responses mediated by Toll, Imd, and Vago in Drosophila remain largely unknow.

To reduce genetic variation due to differences in genetic background, mutant flies were isogenized prior to beginning viral evolution experiments. Homozygous loss-of-function lines for *Dcr-2* (*Dcr-2^{L811fsX}* and *Dcr-2^{R416X}*), *Ago-2* (*Ago-2^{414}*), *spz* (*spz^{2}*), *Dif* (*Dif^{1}*), *Rel* (*Rel^{E20}*), and *Vago* (*Vago$^{\Delta M10}$*) and a hypomorphic mutant line for *Egfr* (*Egfr^{t1}*) were produced in the same genetic background by crossing parental lines at least 10 times to *w^{1118}* flies. Infection phenotypes of the newly produced fly lines were characterized by following their survival after inoculation with DCV by intrathoracic injection (Supplementary Figure 1a). As previously described, *Dcr-2$^{L811fsX/L811fsX}$*, *Dcr-2$^{R416X/R416X}$* and *Ago-2$^{414/414}$* mutants infected with DCV died faster than *w^{1118}* flies[20,21], as well as *Vago$^{\Delta M10/\Delta M10}$*mutants[33]. Toll pathway mutants *spz$^{2/2}$* and *Dif$^{1/1}$* and Imd pathway mutant *Rel$^{E20/E20}$* were less sensitive to DCV infection than *w^{1118}* flies as they died later than *w^{1118}* flies (Supplementary Figure 1a); however, these mutants maintained the previously observed increased susceptibility to infection by Gram + and Gram – bacteria, respectively (Supplementary Figure 1b and 1c). No difference in virus-induced mortality was found between *w^{1118}* and *Egfr$^{t1/t1}$* mutant flies (Supplementary Figure 1a). This set of isogenic mutant flies with

157 contrasting phenotypes to DCV infection provided us with the host model system to
158 perform the viral evolution experiment.
159
160 **Experimental DCV evolution**
161 To study the impact of innate immune pathways on virus population diversity and
162 evolution, DCV from a viral stock was serially passaged (P1 to P10) in w^{1118} flies and
163 in the isogenic innate immune deficient fly lines (Figure 1a and 1b). DCV population
164 diversity was studied after each passage by next generation sequencing (NGS) and
165 DCV virulence was analyzed at the beginning and at the end of the evolution
166 experiment.
167 To follow viral infection during the course of the experiment, viral load ($TCID_{50}$)
168 was determined by end point dilution and prevalence (percentage of flies positive for
169 $TCID_{50}$) was calculated for all passages in individual flies from DCV contaminated
170 cages. We found that for most fly genotypes and for both biological replicates, DCV
171 infection prevailed along the 10 viral passages (Extended Data Figure 1a and 1b).
172 When considering viral loads along passages, only w^{1118}, $Ago\text{-}2^{414/414}$ and $Rel^{E20/E20}$
173 fly lines displayed significant temporal dispersion (Durbin-Watson test for outliers <
174 1.5), consistent among both biological replicates, while viral load in the other fly
175 genotypes remained relatively stable (Durbin-Watson test in the range 1.5 – 2.5) for
176 at least one of the biological replicates (Extended Data Figure 1b). The negative
177 strand of the DCV genome was detected in P10 in all genotypes and biological
178 replicates, confirming that active viral replication occurred for the duration of the
179 evolution experiment (Extended Data Figure 1c). Whether remnants of non-

replicating virus remained in the fly surface was not assessed. Of note, the DCV stock was experimentally introduced to the system only once, to start the P1.

To assess the impact that fly genotype, biological replicate, and viral passage has on viral loads, the log-transformed $TCID_{50}$ values from each fly genotype (Extended Data Figure 1d) were fitted to the generalized linear model (GLM) described in the Materials and Methods section. In short, the model incorporates fly genotype and experimental block as orthogonal factors and passage as covariable. Highly significant differences were observed in viral load among fly genotypes (test of the intercept: χ^2 = 146.734, 8 d.f., $p < 0.001$) that were of very large magnitude (η_P^2 = 84.85%), thus confirming that DCV load strongly varied among host genotypes. A significant effect was also observed for the viral passages (test of the covariable: χ^2 = 5.075, 1 d.f., $p = 0.024$), indicating overall differences in viral accumulation among passages, though the magnitude of this effect was rather small (η_P^2 = 0.28%). Regarding second-order interactions among factors and the covariable, a significant interaction exists between fly genotype and experimental block (χ^2 = 27.082, 8 d.f., $p < 0.001$) indicating that some of the differences observed in virus accumulation among host genotypes differed among biological replicates, and between fly genotype and evolutionary passage (χ^2 = 52.511, 8 d.f., $p < 0.001$). However, despite being statistically significant, these two effects were of very small magnitude (η_P^2 = 2.88% and η_P^2 = 1.49%, respectively), casting doubts about their biological irrelevant. Likewise, the third-order interaction was statistically significant (χ^2 = 86.023, 8 d.f., $p < 0.001$), suggesting that the differences in viral load among experimental blocks observed for a particular host genotype also depended on the evolutionary passages, although once again the effect could be considered as minor (η_P^2 = 1.49%). Next, we

evaluated whether differences exist in viral load between immune competent (w^{1118}) and the different mutant fly genotypes. In all eight cases, DCV accumulated to significantly higher levels in the immune deficient flies than in the wild-type flies ($p < 0.001$), with the smallest significant difference corresponding to viral populations replicating in $Rel^{E20/E20}$ and $Dif^{1/1}$ and the largest to those replicating in $Egfr^{t1/t1}$ and $Dcr\text{-}2^{R416X/R416X}$ (Extended Data Figure 1d).

Overall, these results show that in both immune competent (w^{1118}) and immune deficient flies, DCV oral infection was maintained along passages and confirm that mutant flies are more permissive to DCV infection.

Viral nucleotide diversity increases in the absence of a fully functional immune response

To look into the selective pressure imposed by the Drosophila innate immune pathways on DCV population variation and dynamics, we analyzed virus genome diversity after each passage. Half of the population of infected flies was used to sequence the full-length DCV genome by NGS (Figure 1b and 1c). The viral stocks used to start the experiment, S2 DCV stock and DCV stock, were also sequenced (see Methods section). Analysis of the NGS data was performed using the computational pipeline Viral Variance Analysis (ViVan)[42]. Sequence coverage was at least 8,000 reads per position on the genome. To determine the error rate of the sequencing procedure, including library preparation, four sequencing technical replicates of the S2 DCV stock were used (Supplementary Figure 2). An allele frequency threshold of 0.0028 was used for all subsequent analyses based on variant detection and frequency correlation between technical replicates (see

Methods section). We next calculated the site-averaged nucleotide diversity (π) on all polymorphic sites (n = 1869) across the full-length viral genome and present in the full dataset (Figure 2), with the aim of determining if the lack of activity of a given innate immune pathway had an impact on viral population genetic diversity, in terms of size of the viral mutant swarm.

First, we asked if there was any difference in DCV population diversity and dynamics between the different fly genotypes along the complete evolution experiment. To answer this question, we analyzed if the host genotype, viral passages, biological replicate, or the interactions between these factors had an impact on the evolution of viral population diversity, considering the full-length DCV genome, across all passages. We found that only the fly genotype had a statistically significant impact on π (χ^2 = 25.545, 8 d.f., p = 0.001) (Table 1). We then compared the DCV population diversity present in each fly genotype to each other. We found that, except for viral diversity found in *Dcr-2*$^{L811fs/[L811fsX}$ and *Dif*$^{1/1}$ lines, for which no difference was found compared to π in *w*^{1118} flies ($p \geq 0.303$), DCV population diversity significantly differed from *w*^{1118} line in the rest of the innate immune mutants analyzed ($p \leq 0.013$) (Supplementary Table 1). A *post hoc* Bonferroni test further sorted overlapping groups according to their increasing viral nucleotide diversity: group 1 (less diversity): *w*^{1118}, *Dcr-2*$^{L811fs/[L811fsX}$ and *Dif*$^{1/1}$ fly lines; group 2: *Dif*$^{1/1}$, *Dcr-2*$^{L811fs/[L811fsX}$, *Rel*$^{E20/E20}$, *spz*$^{2/2}$, and *Dcr-2*$^{R416X/R416X}$ fly lines; group 3: *Dcr-2*$^{L811fs/[L811fsX}$, *Rel*$^{E20/E20}$, *spz*$^{2/2}$, *Dcr-2*$^{R416X/R416X}$, and *Ago-2*$^{414/414}$ fly lines; group 4 (more diversity): containing *spz*$^{2/2}$, *Dcr-2*$^{R416X/R416X}$, *Ago-2*$^{414/414}$, *Egfr*$^{t1/t1}$, and *Vago*$^{\Delta M10/\Delta M10}$ fly lines (Extended Data Figure 2 and Supplementary Table 1).

Next, we wondered if the general differences observed in viral nucleotide diversity, between fly genotypes were associated with a particular viral genomic region (*i.e.*, if a determined viral function was affected during the evolution experiment) (Figure 1c). Of note, the intergenic region internal ribosome entry site (IGR IRES) was not included in the analysis because its lack of genetic variation prevented us from determining its nucleotide diversity value. We found that the fly genotype had a statistically significant effect on the nucleotide diversity found in each DCV genomic region (χ^2 = 27.178, 8 d.f., $p < 0.001$), which further differed between each specific viral genomic region (χ^2 = 11.698, 8 d.f., $p = 0.008$). As a second-order interaction, an effect of the fly genotype and the biological replicate was found (χ^2 = 16.314, 8 d.f., $p = 0.038$) (Table 1). Comparison of viral genetic diversity within the genomic regions allowed us to distinguish three main groups: group 1 (less diversity): 3'UTR; group 2: 5'UTR IRES; and group 3 (more diversity): ORF1 and ORF2 (Extended Data Figure 2 and Supplementary Table 1).

Finally, we wondered if viral diversity evolved from the starting viral stock (DCV stock) in each fly genotype. π present in P1, P5 and P10 was compared between fly genotypes and with the diversity present in the DCV stock. We found that pairwise comparisons of viral nucleotide diversity present in each fly genotype in P1, between each other and versus DCV stock, yield no statistically significant difference ($p = 1.000$) (Supplementary Table 1). In P5 viral diversity was reduced only in w^{1118} (Group 1/2; $p = 0.026$ and $p = 0.032$) compared to the starting viral stock (Extended Data Figure 2 and Supplementary Table 1). In P10, viral nucleotide diversity present in w^{1118} (Group 1; $p = 0.032$ and $p = 0.041$), $spz^{2/2}$ (Group 1; $p = 0.020$ and $p = 0.025$), $Dif^{1/1}$ (Group 1; $p = 0.005$ and $p = 0.006$) and $Rel^{E20/E20}$ (Group 1/2; $p = 0.046$)

mutant flies was reduced when compared to DCV diversity from the DCV stock (Extended Data Figure 2 and Supplementary Table 1).

Altogether, the results show that the absence of a fully functional immune system results in an increase of viral population diversity that remains constant along passages. They also show that the coding regions of the virus are more prone to accumulate variation than the non-coding regions where regulatory elements are present.

Viral population diversity derives from preexisting standing genetic variation

Next, we examined if the levels of viral diversity observed in DCV populations from innate immune mutants compared to the w^{1118} line were accompanied with the fixation of particular genetic changes in the mutant swarms, and whether (*i*) whether these changes can be associated with fitness effects and (*ii*) whether potentially adaptive mutations arose in response to particular immune responses. To do so, we estimated the selection coefficients for each SNP using their variation in frequency across evolutionary time (Figure 3 and Extended Data Figure 3), using a classic population genetics approach[43] (Table 2). Thirty-six SNPs yielded significant estimates of selection coefficients (this number reduces to 10 if a stricter FDR correction is applied; Table 2). Twenty-one of them were already detected in the ancestral S2 DCV stock, henceforth a maximum of 15 new SNPs might have arisen during the evolution experiment. Estimated selection coefficients for all these SNPs ranged between −0.304 per passage (synonymous mutation RdRp/C5713U) and 1.204 per passage (VP2/G6311C nonsynonymous change R16P), with a median value of 0.286 per passage (interquartile rank = 0.265). Nine mutations were

observed in more than one lineage (range 2 - 7 linages), with synonymous mutations VP3/U7824C appearing in seven lineages of six different host genotypes and mutation 5'UTR/A280U in five lineages of five host genotypes (Table 2). These nine SNPs were all present in the S2 DCV stock. Indeed, the frequency of SNPs among evolving lineages is significantly correlated with their frequency in the ancestral S2 DCV stock (Pearson's $r = 0.401$, 36 df, $p = 0.013$), but not with their measured fitness effect ($r = -0.091$, 36 df, $p = 0.588$).

An interesting question is whether the fitness effects associated with each of these nine SNPs were the same across all genotypes or, conversely, whether fitness effects were host genotype-dependent. To test this hypothesis, we performed one-way ANOVA tests comparing fitness effects (Table 2) across the corresponding host genotypes. In all cases, significant differences were observed ($F \geq 15.637$ and $p \leq 0.001$, and $\geq 93.99\%$ of total observed variance in fitness effects explained by true genetic differences among host genotypes), supporting the notion that fitness effects are indeed host-genotype dependent. A pertinent example is the case of the synonymous mutation VP3/U7824C, which was the most prevalent mutation ($F_{6,45} = 158.862$, $p < 0.001$, 99.37% of genetic variance). In this case, a *post hoc* Bonferroni test shows that host genotypes can be classified into three groups according to the fitness effect of this SNP. In genotypes $Dcr\text{-}2^{R416X/R416X}$ and $Rel^{E20/E20}$, the mutation has a deleterious effect (on average, −0.2260 per passage); in genotypes $Egfr^{t1/t1}$ and $Vago^{\Delta M10/\Delta M10}$, the mutation is moderately beneficial (on average, 0.1257 per passage; and in genotypes w^{1118} and $Ago\text{-}2^{414/414}$, the mutation had a strong beneficial effect (on average, 0.502 per passage).

As shown in Figure 3 and Extended Data Figure 3a, some SNPs show a strong parallelism in their temporal dynamics, suggesting they might be linked into haplotypes. This is particularly relevant for mutations shown in Table 2. To test this possibility, we computed all pairwise Pearson correlation coefficients between mutation frequencies along evolutionary time. The results of these analyses are shown in Extended Data Figure 3b to 3k as heatmaps. Again, as an illustrative example, we discuss here the case of the viral population BR2 evolved in *Ago-2*$^{414/414}$ (Extended Data Figure 3d). Synonymous mutations VP3/U7824C and VP1/C8424U and nonsynonymous mutation VP1/C8227U (H655Y) are all linked into the same haplotype ($r \geq 0.998$, $p < 0.001$). Since these three mutations already existed in the S2 DCV stock, it is conceivable that the haplotype already existed and has been selected as a unit. Indeed, the fitness effects estimated for these three mutations are indistinguishable (one-way ANOVA: $F_{2, 22} = 1.781$, $p = 0.192$; average fitness effect 0.590 $\pm$0.032 per passage), thus suggesting that the estimated value corresponds to the haplotype as a unit. The absence of this haplotype in *Ago-2*$^{414/414}$ BR1 suggests it was lost during the transmission bottleneck from S2 cells to flies. Interestingly, mutations VP1/C8424U VP1/C8227U appear also linked into the same haplotype in population BR2 evolved in *Dcr-2*$^{L811fsX/L811fsX}$ (Extended Data Figure 3b). These two cases, as well as populations BR1 evolved in *Rel*$^{E20/E20}$, BR2 evolved in *spz*$^{2/2}$ and BR1 and BR2 evolved in *Vago*$^{\Delta M10/\Delta M10}$ illustrate some examples of haplotypes (Extended Data Figure 3f, 3e, 3h, and 3i). Other viral populations, especially those evolved in *Egfr*$^{t1/t1}$ flies, show much more complex patterns (Extended Data Figure 3j and 3k) in which haplotypes change over time by acquiring *de novo* mutations.

345 When mapping the 36 SNPs found to have significant estimates of selection
346 coefficients in the viral genome (Table 2 and Extended Data Figure 4), we found that
347 two mapped to the 5'UTR IRES, twelve to ORF1, one to the IGR IRES, 20 to ORF2,
348 and one to the 3'UTR. Of the twelve mutations observed in ORF1, which encodes the
349 non-structural proteins, four mapped to the 3C viral protease and five to the RdRp.
350 Only one of these mutations in the 3C viral protease was non-synonymous. Of the 20
351 mutations in ORF2, which encodes the viral structural proteins, eight mapped to VP2,
352 five to VP3, and seven to VP1. These correspond to the three majors predicted DCV
353 capsid proteins.
354 Taken together, these results show that viral population diversity over these
355 ten *in vivo* passages mainly derived from preexisting standing genetic variation in the
356 ancestral DCV population. Furthermore, temporal dynamics of population diversity
357 were linked to the fly genotype in which the virus evolved.
358
359 **DCV virulence decreases along passages in the absence of immune pathways**
360 Finally, we wondered if DCV virulence varied among each lineage in the different fly
361 genotypes. Infectious DCV stocks were produced from viral passages P1 and P10
362 and from all fly genotypes. Because the viral evolution experiment was performed by
363 DCV orofecal transmission, we first evaluated DCV virulence by feeding w^{1118} flies
364 with DCV stocks derived from P1 or P10; survival was evaluated from each fly
365 genotype. We found that only a small proportion of flies (between 5% and 20%)
366 succumbed to DCV infection, and no statistically significant differences in mortality
367 were found between mock and virus infected flies, regardless of viral passage or fly
368 genotype (Supplementary Figure 3). This is in agreement with previously published

works showing that DCV oral infections are cleared in w^{1118} flies[31]. We next decided to investigate the evolution of virulence by intrathoracic inoculation of DCV stocks. We found that w^{1118} flies were less sensitive to viral infection when inoculated with DCV stocks derived from P10 since their median survival time was longer than those inoculated with stocks from P1 for most DCV stock origins (Figure 4a and Supplementary Table 2). Notable exceptions were DCV stocks from BR2 of $Vago^{\Delta M10/\Delta M10}$ mutant flies, for which w^{1118} flies were more sensitive to P10 than to P1, and stocks from BR1 of $spz^{2/2}$ and BR2 of $Egfr^{t1/t1}$ mutant flies, for which no difference in median survival time after infection with DCV between P1 and P10 was detected.

A fundamental question in evolutionary biology is the role that past evolutionary events may have in the outcome of evolution[44]. If ongoing evolution is strongly contingent with past evolutionary events, ancestral phenotypic differences should be retained to some extent, while if other evolutionary forces such as selection and stochastic events (*i.e.*, mutation and genetic drift) dominate, then ancestral differences can be eroded and, in the extreme case, even fully removed. Here, we observed significant differences in the performance of the ancestral DCV across the eight host genotypes. To test whether these differences are still observable in the evolved population, we compared the median survival time (Figure 4a and Supplementary Table 2) for DCV populations isolated at the beginning of the evolution experiment P1 and at the end P10 (Figure 4b). Under the null hypothesis of strong historical contingency, it is expected that data will fit to a regression line of slope 1 and intercepting the ordinate axis at 0. However, if ancestral differences have been removed, data would fit significantly better to a regression line with a slope

393 smaller than one and with an intercept greater than zero[44]. Figure 4b shows the data
394 and its fit to the null hypothesis (solid black line) and the alternative hypothesis
395 (dashed red line). A partial *F*-test shows that adding an intercept to the regression
396 equation significantly improves the fit ($F_{1,16} = 28.437$, $p < 0.001$), thus supporting the
397 notion that ancestral differences among host genotypes have been removed by the
398 action of subsequent adaptation, that is, the fixation of beneficial mutations.
399
400 **Discussion**
401 In this work we aimed at determining the overall impact of innate immunity on viral
402 evolution. Based on the arms-race hypothesis, we speculated that if a given host
403 defense mechanism imposes a specific selective pressure on a particular pathogen
404 function, the absence of this defense mechanism would result in the relaxation of the
405 selective constraint, which would in turn be detectable in the pathogen at the
406 genomic and phenotypic levels. We found that viral population diversity evolved
407 differently according to each fly genotype; however, viral population diversity mostly
408 derives from ancestral standing genetic variation (*i.e.*, few "new" mutations were
409 selected). Our results further confirm the polygenic nature of antiviral responses;
410 there is not a specific, main immune defense mechanism against a particular virus,
411 but instead a repertoire of defense mechanisms that are triggered after infection and
412 that might interact with each other.
413 Our results are compatible with a pervasive presence of clonal interference. In
414 the absence of sexual reproduction, clonal interference is the process by which
415 beneficial alleles originated in different clades within a population compete with each
416 other, resulting in one of them reaching fixation. Subsequently, the outcompeted

beneficial allele may appear in the new dominant genetic background and, assuming no negative epistasis among both loci, become fixed. As a consequence, beneficial mutations may fix sequentially, thus slowing down the rate of adaptation[45]. Given their large effective population size and high mutation rates, viral populations are expected to contain considerable amounts of potentially beneficial standing variation, making them prone to clonal interference. Indeed, it has been previously shown to operate in experimental populations of vesicular stomatitis virus adapting to cell cultures[46,47], in bacteriophage ϕX174 populations adapting to harsh saline environments[48], in tobacco etch virus adapting to novel plant host species[49], among HIV-1 escape variants within individual patients[50], and also at the epidemiological level among influenza A virus lineages diversifying antigenically[51]. In our own results, clonal interference can be observed in populations BR1 evolved in *Dcr-2*$^{L811fsX/L811fsX}$, BR1 evolved in *Ago-2*$^{414/414}$, BR1 evolved in *spz*$^{2/2}$, BR2 evolved in *Rel*$^{E20/E20}$, and BR2 evolved in *Vago*$^{\Delta M10/\Delta M10}$. All of these viral populations share similar patterns in which some beneficial allele (or haplotypes) rose in frequency, reached a peak at some intermediate passage, then declined in frequency and were finally outcompeted by a different beneficial mutation (or haplotype) that had lower initial frequency. For example, the nonsynonymous mutation VP2/G6931A (A223T) appeared *de novo* in population BR1 evolved in *spz*$^{2/2}$, and outcompeted several mutations likely linked in a haplotype (Figure 3). Tightly linked to clonal interference is the concept of leap-frogging[52], in which the beneficial mutation that ends up dominating the population is less genetically related to the previously dominant haplotype than to the common ancestor of both (Figure 3). The VP2/G6931A mutation illustrates this case well, as it appeared in a genetic background that was

441 minoritarian rather than in the dominant one. Likewise, the mutation VP2/G6311C
442 (R16P), observed in BR1 evolved in *w*^{1118} flies, appeared in a low frequency genetic
443 background different from the most abundant one in previous passages. Finally, the
444 haplotype containing five different mutations observed in BR2 evolved in *spz*$^{2/2}$
445 became dominant in frequency after P6, outcompeting two other mutations that were
446 dominating the population until then.

447 The existence and fixation of haplotypes along our evolution experiment
448 deserves further discussion. Linked mutations generate three possible interference
449 effects[53]. First, all mutations might contribute additively, or may be involved in
450 positive epistasis, to the fitness of the haplotype as a whole, thus increasing its
451 chances to become fixed. Second, hitchhiking and genetic draft may occur, by which
452 deleterious or neutral alleles are driven to fixation along with a linked beneficial allele.
453 Third, there may be background selection by which the spread of a beneficial allele is
454 impeded, or at least delayed, owing to the presence of linked deleterious alleles. For
455 instance, we can hypothesize that haplotype VP3/U7824C-VP1/C8227U-
456 VP1/C8424U, which swept to fixation in population BR2 evolved in *Ago-2*$^{414/414}$, may
457 represent a case of genetic draft: two synonymous mutations, potentially neutral,
458 linked to a nonsynonymous one that may be the actual target of selection. Yet, the
459 lack of an infectious clone for DCV does not allow us to test this hypothesis.

460 Some of the mutations we found to be associated with positive selection
461 coefficients were synonymous changes (Table 2). However, equating synonymous
462 mutations with neutral mutations in compacted RNA genomes has proven to be
463 misleading[54,55]. Selection operates at different levels of a virus's infection cycle, and
464 not all these levels necessarily depend on the amino acid sequence of encoded

proteins. For instance, a lack of matching between virus and host codon usages would slowdown translational speed and efficiency[56]; mutations affecting the folding of regulatory secondary structures at noncoding regions would affect the interaction with host and viral factors and thus impact the expression of downstream genes (*e.g.*, mutations 5'UTR/A280U, IGR/A6108G and 3'UTR/U9163A all with significant fitness effects -Table 2)[57]; or evasion from antiviral RNAi defenses by changing the most important relevant sites in the target of siRNAs[12,13].

It is interesting to observe that viral diversity in mutants for antiviral RNAi, whose mode of action relies on a direct interaction with the viral genome, did not display increased diversity when compared to mutants from the other immune pathways. One could expect that the release of the selective pressure that RNAi exerts on the virus genome may allow for the appearance of mutations in the viral suppressor of RNAi. Nonetheless, we did not observe such a change, possibly because the RNAi suppressor in DCV shares the first 99 amino acids of the RdRp[58,59] and mutations would affect polymerase activity. The antiviral action of the other immune pathways remains still unknown and may even be indirect; for example the known roles of Imd, Toll, and Egfr pathways in controlling fly microbiota[38,39] might possibly affect the prevalence of virus infections. In this regard, it is important to highlight that the diversity of DCV in the *Dif*$^{1/1}$ mutant (Toll pathway, already described not to have an impact on DCV defense[25]), was indistinguishable from *w*^{1118}, pointing to the specific - although uncharacterized - antiviral functions of the other immune pathways.

Another consideration when interpreting our results is the nature of the virus stock used. This virus stock has been maintained for years in Drosophila S2 cells.

The observation that viral population diversity decreased along passages in w^{1118} flies, highlights the strength of the selective forces that constrain the virus from adapting to a new environment. During the successive passages, in the absence of a given immune response, the capacity of the virus to evolve will be determined by a combination of two factors: the adaptation to the new environment (constraining factor) and the lack of immune response (relaxation factor). Because DCV replication is significantly increased in immune deficient mutants, the potential for population diversification is higher. This effect is clearly observed in w^{1118} flies where the virus is "only" adapting to the new environment and DCV populations evolved in w^{1118} flies show less variation than all other lineages. Future experimental evolution studies using viral stocks derived from flies, instead of cell cultures, are warranted to address this topic.

In a study published recently[60], Navarro *et al.* used *Arabidopsis thaliana* and turnip mosaic virus to carry out experimental virus evolution assays with a similar design to ours. In their work, the authors used plant mutants compromised in their antiviral response (more permissive to viral infection) or with an enhanced antiviral response (less permissive to viral infection) and allowed the virus to evolve for 12 passages. Similarly to what we found in the *D. melanogaster* - DCV system, the authors showed that viral population evolutions dynamics, as well as viral loads, depend on host genotype. Interestingly, a reduction of ancestral genetic variation regardless of the immune pathway affected was also clearly observed, in agreement with our observations.

Taken together, our results point to the concerted action of the different immune pathways to limit viral evolution. Response to infection does not simply

consist of activating immune pathways, it also encompasses a broad range of physiological consequences including metabolic adaptations, stress responses and tissue repair. Critically, upon infection, the homeostatic regulation of these pathways is altered. However, such alterations do not always result in increased disease severity and in fact can even lead to improved survival (or health) despite active virus replication.

Materials and Methods

Fly strains and husbandry

Flies were maintained on a standard cornmeal diet (Bloomington) at a constant temperature of 25 °C. All fly lines were cleaned of possible chronic infections (viruses and Wolbachia) as described previously[61]. The presence or absence of these chronic infections was determined by RT-PCR with specific primers for Nora virus, Drosophila A virus, DCV (NoraVfor ATGGCGCCAGTTAGTGCAGACCT, NoraVrev CCTGTTGTTCCAGTTGGGTTCGA DAVfor AGAGTGGCTGTGAGGCAGAT, DAVrev GCCATCTGACAACAGCTTGA, DCVfor GTTGCCTTATCTGCTCTG, DCVrev CGCATAACCATGCTCTTCTG) and by PCR with specific primers *Wolbachia sp* (wspfor TGGTCCAATAAGTGATGAAGAAAC, wsprev AAAAATTAAACGCTACTCCA and wspBfor TTTGCAAGTGAAACAGAAGG, wspBrev GCTTTGCTGGCAAAATGG).

Fly mutant lines *Dcr-2*^{L811fsX} and *Dcr-2*^{R416X} [62], *Ago-2*^{414} [63], *Spz*^{2} [64], *Dif*^{1} [65], *Rel*^{E20} [66], *Vago*$^{\Delta M10}$ [33]and *Egfr*^{t1} [67] were isogenized to *w*^{1118} fly line genetic background first by replacing the chromosomes not containing the mutation using

balancer chromosomes and then by recombination by backcrossing at least ten times to w^{1118} line. The presence of the mutation was followed during and at the end of the backcrossing procedure by PCR and sequence analysis using specific primers (Dcr2811_3001for TTTGACCCATGACTTTGCGGT, Dcr2811_3294rev CCTTGCAGAGATGCCCCTGTT, Dcr2416_4341for GATTGGCATTACCGTCCCGAA, Dcr2416_4670rev AGCGATTCCTG ATGAGTCTTA, Ago2414_rev TTGTGGATGGCTGTTGTCTCG, Ago251B414_for AGAGTCCCCACTTGAATGGCC, Spz2_for GCCTTTGGCGCTTGCCTAATT, Spz2_rev GCTCCTGCAAAGGAATCGCTC, Dif1_for CTTGGCAATCTTCTCGCACAG, Dif1_rev ATCGTGGTCTCCTGTGTGACG, Rel_Ex4rev AGCTCTCCAGTTTGTGCCGAC, Rel-RD_5'UTRfor CTGGCGTTAGTTTCGGCGTTG, Vagod10_for TTGGCCAACGGAAAGGATGTG, Vagod10_rev TGCCACCGATGATCAATGACA, Egfrt1_for CAAAGCTCGAACCGAAATTA, Egfrt1_rev CTTTCTTAACGTCCACATGA).

Virus production and titration

The S2 DCV stock used to start the experiment was prepared in S2 cells. Cells were maintained in Schneider culture medium and at 25 °C and observed daily. Cells were harvested when cytopathic effects were detected, then frozen at –80 °C, thawed on ice and centrifuged for 15 min at 15,000 g at 4 °C. The supernatant was recovered, aliquoted and stored at –80 °C. Viral stocks were tittered in S2 cells, determined using the end-point dilution method and expressed as fifty-percent tissue culture infective dose ($TCID_{50}$)[68].

560 To produce the DCV stocks from passages P1 and P10 from the evolution
561 experiment half of the population of flies infected with DCV from each fly genotype
562 (approx. 250 flies) was homogenized in 1× PBS, homogenates were frozen at –80
563 °C, then thawed on ice, centrifuged to discard the tissue debris, supernatant was
564 recovered and filtered to discard bacteria contamination, then aliquoted and stored at
565 –80 °C. Viral stocks were tittered in S2 cells using the end-point dilution method and
566 expressed as fifty-percent tissue culture infective dose ($TCID_{50}$).
567
568 **Viral and bacterial infections and survival analysis**
569 To characterize the isogenized fly lines, 4 to 5 day old female flies were
570 intrathoracically injected with a Nanoject II apparatus (Drummond Scientific) with 50
571 nl of the pathogen suspension. For DCV infections, a suspension of 10 $TCID_{50}$ units
572 of DCV in 10 mM Tris buffer, pH 7 was used. An injection of the same volume of 10
573 mM Tris, pH 7 served as a mock-infected control. Infected flies were kept at 25 °C,
574 transferred into fresh vials every 2 days and number of dead flies was scored daily.
575 For bacterial infections, 50 nl of suspensions in 1× PBS buffer, pH 7, of optical
576 density (OD) = 10 for *Enterococcus faecalis*, and of OD = 200 for *Erwinia carotovora*
577 *carotovora 15* (Ecc15) were used. An injection of the same volume of 1× PBS buffer
578 served as a mock-infected control. Flies infected with *E. faecalis* were kept at 25 °C,
579 and flies infected with Ecc15 were kept at 29 °C. Flies were transferred into fresh
580 vials every 2 days and number of dead flies was scored daily.
581
582 **Virus experimental evolution**

583 To produce the starting DCV stock (DCV stock) 5 to 6 days old w^{1118} female flies
584 were intrathoracically injected with 100 $TCID_{50}$ of DCV from a stock produced in S2
585 Drosophila cells (S2 DCV stock) or mock infected. At 4 dpi, $N = 90$ DCV infected flies
586 (DCV stock) were placed in cages containing fresh medium, left for 3 days and then
587 removed to place in this DCV-or mock-contaminated cages $N = 500$ 5-to-6-day old
588 wild type or mutant flies (males and females). Flies were allowed to feed ad libitum
589 for 3 days (oral inoculation period), then moved to a clean cage for 1 day, and further
590 placed into a new clean cage and left for 4 days, when they were harvested (P1). A
591 new group of flies was then placed into the contaminated cages. This procedure was
592 repeated 10 times (10 DCV Passages, P1 to P10) and replicated twice (biological
593 replicates BR1 and BR2). The total amount of flies from each passage, fly genotype,
594 and biological replicate was collected and randomly divided in halves (approx. 250
595 flies), one half was used to extract total RNA and produce the NGS libraries and the
596 other half to produce viral stocks to evaluate DCV virulence.
597
598 **Characterization of infection during passages**
599 Individual flies from each passage were anesthetized and homogenized in 100 ml of
600 1´ PBS buffer. The tubes containing the homogenates were centrifuged for 5 min at
601 15,000×g at 4 °C to discard the tissue debris. The supernatant was recovered and
602 used to determine viral load ($TCID_{50}$) by end point dilution and prevalence
603 (percentage of flies positive for $TCID_{50}$) for each fly genotype, viral passages and
604 biological replicate.
605 For statistical analyses, $TCID_{50}$ data were transformed as $T = \log(TCID_{50} + 1)$
606 and then fitted to a generalized linear model in which fly genotype (G) and BR (B)

were treated as orthogonal factors. *G* was considered as a fixed effects factor whereas *B* was considered as a random effects factor. Evolutionary passage (*P*) was introduced in the model as a fixed effects covariable. We also considered second and third order interactions between the two factors and the covariable. The model equation thus reads:

$$T_{ijk}(P) \sim \tau + P + G_i + B_j + (P \times G)_i + (P \times B)_j + (G \times B)_{ij} + (P \times G \times B)_{ij} + \varepsilon_{ijk}.$$

Where $T_{ijk}(P)$ is the transformed $TCID_{50}$ observed for a particular titration assay *k* of BR *j* of fly genotype *i*, τ represents the grand mean value and ε_{ijk} stands for the error assumed to be Gaussian distributed at every *P*. The significance of each term in the model was evaluated using a likelihood ratio test that follows a χ^2 probability distribution. The magnitude of the effects was evaluated using the η_P^2 statistic (proportion of total variability in the traits vector attributable to each factor in the model; conventionally, values of $\eta_P^2 \geq 0.15$ are considered as large effects). These analyses were done using SPSS version 27 (IBM, Armonk, NY).

Detection of negative strand DCV RNA by strand-specific RT-qPCR (ssRT-qPCR)

To determine the amount of negative strand DCV RNA present in the viral stocks produced from each fly genotype in P10, S2 DCV stock, and DCV stock, total RNA was extracted from the DCV stocks produced from P10 (all fly genotypes, both biological replicates) and from the DCV stocks used to start the experiment. ssRT-qPCR was performed with these RNA samples essentially as described[35]. We used 800 ng of RNA to perform reverse transcription with SuperScript II reverse transcriptase (Invitrogen) according to the manufacturer's instructions, with the

631 exception that primer annealing occurred at 70 °C and cDNA synthesis occurred at
632 50 °C for 30 minutes. Reverse transcription was performed using a forward primer
633 containing a non-target tag sequence (DCV_tag_F:
634 AATTCAAGCTCGTCTTCCTCGAGGCTGTGTTTGCGCGAAG) A standard curve
635 was produced by reverse transcription of a tenfold dilution series (from 10^8 to 10^3
636 copies per reaction) of *in vitro* transcribed RNA corresponding to a portion of the full-
637 length negative strand DCV RNA. Following reverse transcription, cDNA was diluted
638 1:10 and used for for qPCR with the Luminaris Color HiGreen low ROX qPCR Master
639 Mix (Thermo Scientific) according to the manufacturer's instructions. A forward
640 primer containing the non-target tag sequence (Tag_qPCR_F:
641 AATTCAAGCTCGTCTTCCTCG) and a a DCV-specific reverse primer
642 (DCV_qPCR_R: AATGGCAAGCGCACACAATTA) were used for qPCR.
643
644 **RNA extraction, cDNA synthesis and NGS library production**
645 To produce the NGS libraries from the evolution experiment, half of the total
646 population of flies infected with DCV from each fly genotype, viral passage and
647 biological replicates (approx. 250 flies) was used. To produce the NGS libraries from
648 the viral stock from S2 cells (S2 DCV stock), two different aliquots of the stocks were
649 used. To produce the NGS libraries from the DCV stock (virus infecting w^{1118} female
650 flies used to contaminate the cages to start the evolution experiment), half of the
651 population of the infected flies (approx. 800 flies: N = 90 flies/cage ´ 9 fly genotypes ´
652 2 BR) was used. In all cases, total RNA was extracted using TRIzol reagent
653 (Invitrogen) following the manufacturer's instructions and the final concentration was
654 determined using a NanoDrop ND-1000 Spectrophotometer. 300 ng of total RNA

were used to produce the cDNA using oligo(dT) as primers reverse transcription with the Maxima H Minus Reverse Transcriptase Kit (Thermo Fisher Scientific) according to manufacturer's instructions. The cDNA obtained served as template to amplify the full-length genome of DCV with specific primers (DCVfor ATATGTACACACGGCTTTTAGGT and DCVrev CAGTAAGCAGGAAAATTGCG) using Phusion High-Fidelity DNA polymerase Kit (Thermo Fisher Scientific) in the following conditions: initial denaturation at 98 °C for 30 seconds; 30 cycles of denaturation at 98 °C for 10 seconds, annealing at 55 °C for 30 seconds and extension at 72 °C for 5 minutes; and final extension at 72 °C for 10 minutes. For both S2 DCV stock and DCV stock, four different DCV PCR amplifications were done to produce a total of four technical replicates of the NGS libraries. The PCR products were gel purified using the NucleoSpin Gel and PCR Clean-up kit (Machery-Nagel) and their concentration was determined using a NanoDrop ND-1000 Spectrophotometer. 200 ng of the purified PCR product were fragmented into 200 to 300 nucleotides long products using an LE220 ultrasonicator (Covaris) following the manufacturer's instructions. The obtained fragments were used to produce the NGS library using the NEBNext UltraII DNA Library Prep Kit for Illumina (New England BioLabs), according to manufacturer's instructions. The quality of the libraries was verified using a High Sensitivity DNA Chip (Agilent) and quantified using the Quant-iT DNA assay kit (Thermo Fisher Scientific). A 1 nM dilution of the libraries was used for the sequencing that was performed on a NextSeq sequencer (Illumina) with a NextSeq 500 Mid Output kit v2 (Illumina) (151 cycles). Two of the four technical replicates for S2 DVC stock and DCV stock were included in each run.

678 Sequencing of DCV populations from *Dif*$^{1/1}$ mutant flies from P4 and P6 from
679 BR1 and P8 from BR2 did not work.
680
681 **Genetic diversity analyses**
682 **Variant frequency threshold.** To determine the error rate of the sequencing
683 procedure, including library preparation, four sequencing technical replicates from S2
684 DCV stock were used (Supplementary Figure 3a). First, pairwise comparison was
685 done to identify the variant frequency threshold above which at least 95% of the
686 variants were detected in both considered replicates (highest detection threshold =
687 0.0028). All variants above detection threshold were then correlated between each
688 technical replicate to ensure good correlation between reported frequency values: the
689 Pearson correlation coefficient between the detected frequency for variants was $r \geq$
690 0.982 for all pairwise correlation ($p < 0.001$). The R packages used for these analysis
691 were somewhere else described[69–72].
692
693 **Nucleotide diversity (π).** Nucleotide diversity of the viral population was computed
694 using the following formula[73]:
695 $$\pi = \frac{D}{D-1}\{1 - [p^2 + (1-p)^2]\}$$
696 with *D*, the sequencing depth and *p* the frequency of the minority variant at each
697 nucleotide site. For diallelic SNV, π ranges from 0 to 0.5 (both alleles at equal
698 frequency). In the subsequent analyses, π was averaged over all polymorphic
699 nucleotide sites of the DCV genome of each sample[74]. A site was considered
700 polymorphic if at least one sample showed the presence of a nucleotide variant at
701 said position of the DCV genome. Log_{10}-transformed site-averaged π values were

then compared between fly genotypes (orthogonal factor), biological replicates (orthogonal factor), passages (continuous variable) and genomic regions (orthogonal factor) and their interactions using a generalized linear model. The significance of each term in the model was evaluated using a likelihood ratio test that follows a χ^2 probability distribution.

Estimation of relative mutational fitness effects. We have followed the classic population genetics method described in Hartl and Clark (1989)[43]. In short, lets $x_l(t)$ be the frequency of a mutant allele (SNP) at genomic position l and passage t and, therefore, $1 - x_l(t)$ the frequency of the wild-type allele. It holds that $\log \frac{x_l(t)}{1-x_l(t)} = \log \frac{x_l(0)}{1-x_l(0)} + t\log(1 - s_l)$, where s_l is the selection coefficient of the mutant relative to the wild-type allele at locus l. Selection coefficients calculated this way have units of inverse time (per passage in our case). This equation was fitted to the time series data of each locus l shown in Figure 3 by least squares regression, obtaining an estimate of s_l and its standard error (SEM).

Haplotype inference was done using two different statistical approaches. First, by assessing the similarity between temporal dynamics of all possible pairs of loci. To this end, Pearson partial correlation coefficients (controlling for passages) were computed and their significance level corrected for multiple tests of the same null hypothesis using Benjamini and Hochberg (1995)[75] false discovery rate (FDR) method. Correlation coefficient matrices were visualized as heatmaps in which more similar alleles were clustered together. Second, we confirmed the results from the first method using the longitudinal variant allele frequency factorization problem (LVAFFP) method as implemented in CALDER[76]. LVAFFP generates spanning trees

of a directed graph constructed from the variant allele frequencies. The output of CALDER was used as input of TimeScape[77] to generate the Muller plots that illustrate the ancestry of mutations and haplotypes along the evolution experiment (Figure 3).

Statistical analyses described in this section have been done with R version 4.0.2 in RStudio version 1.3.1073.

Data availability

All raw data from high-throughput sequencing were deposited to NCBI BioProjects under accession number PRJNA782868.

Code availability

Scripts are provided in Supplementary Data 1.

Acknowledgements

We thank members of the Saleh Lab, M. Vignuzzi and J. Pfeiffer for fruitful discussions. We thank C. Meignin for *Rel*^{E20} and *Vago*$^{\Delta M10}$ flies. This work was supported by the European Research Council (FP7/2013–2019 ERC CoG 615220) and the French Government's Investissement d'Avenir program, Laboratoire d'Excellence Integrative Biology of Emerging Infectious Diseases (grant ANR-10-LABX-62-IBEID) to M.-C.S. Work in S.F.E.'s laboratory was supported by grants BFU2015-65037-P and PID2019-103998GB-I00 (Spain Agencia Estatal de Investigación - FEDER) and PROMETEU2019/012 (Generalitat Valenciana).

Author contributions

V.M. and M.-C.S. conceived the study, and V.M., M.-C.S., A.K. and L.Q-M. established the experimental design. V.M., V.G., H.B, and J.N. performed the investigations. S.L. and S.F.E. performed the formal analyses. V.M., S.F.E. and M.-C.S. wrote the paper and acquired funding.

Competing interests

The authors declare no competing interests.

Materials & Correspondence: carla.saleh@pasteur.fr to whom correspondence and material requests should be addressed.

References

1. Morgan, A. D. & Koskella, B. Coevolution of Host and Pathogen. in *Genetics and Evolution of Infectious Diseases* 115–140 (Elsevier, 2017). doi:10.1016/B978-0-12-799942-5.00006-8.

2. Daugherty, M. D. & Malik, H. S. Rules of Engagement: Molecular Insights from Host-Virus Arms Races. *Annu. Rev. Genet.* **46**, 677–700 (2012).

3. Barreiro, L. B. From evolutionary genetics to human immunology: how selection shapes host defence genes. *G E N E Ti C S* 14.

4. Thompson, J. N. & Burdon, J. J. Gene-for-gene coevolution between plants and parasites. **360**, 5 (1992).

5. Buckling, A. & Rainey, P. B. Antagonistic coevolution between a bacterium and a bacteriophage. 6 (2002).

6. Masri, L. *et al.* Host–Pathogen Coevolution: The Selective Advantage of Bacillus thuringiensis Virulence and Its Cry Toxin Genes. *PLOS Biol.* **13**, e1002169 (2015).

7. Obbard, D. J., Gordon, K. H. J., Buck, A. H. & Jiggins, F. M. The evolution of RNAi as a defence against viruses and transposable elements. *Philos. Trans. R. Soc. B Biol. Sci.* **364**, 99–115 (2009).

8. Lazzaro, B. P. Natural selection on the Drosophila antimicrobial immune system. *Curr. Opin. Microbiol.* **11**, 284–289 (2008).

9. Lazzaro, B. P. Molecular Population Genetics of Inducible Antibacterial Peptide Genes in Drosophila melanogaster. *Mol. Biol. Evol.* **20**, 914–923 (2003).

10. Sackton, T. B. *et al.* Dynamic evolution of the innate immune system in Drosophila. *Nat. Genet.* **39**, 1461–1468 (2007).

11. Brackney, D. E., Beane, J. E. & Ebel, G. D. RNAi Targeting of West Nile Virus in Mosquito Midguts Promotes Virus Diversification. *PLoS Pathog.* **5**, 9 (2009).

12. Lin, S.-S. *et al.* Molecular Evolution of a Viral Non-Coding Sequence under the Selective Pressure of amiRNA-Mediated Silencing. *PLoS Pathog.* **5**, e1000312 (2009).

13. Lafforgue, G. *et al.* Tempo and Mode of Plant RNA Virus Escape from RNA Interference-Mediated Resistance. *J. Virol.* **85**, 9686–9695 (2011).

14. Martínez, F. *et al.* Ultradeep sequencing analysis of population dynamics of virus escape mutants in RNAi-mediated resistant plants. *Mol. Biol. Evol.* **29**, 3297–3307 (2012).

15. Das, A. T. *et al.* Human Immunodeficiency Virus Type 1 Escapes from RNA Interference-Mediated Inhibition. *J. Virol.* **78**, 2601–2605 (2004).

16. Gitlin, L., Stone, J. K. & Andino, R. Poliovirus Escape from RNA Interference: Short Interfering RNA-Target Recognition and Implications for Therapeutic Approaches. *J. Virol.* **79**, 1027–1035 (2005).

17. Mondotte, J. A. & Saleh, M.-C. Antiviral Immune Response and the Route of Infection in Drosophila melanogaster. in *Advances in Virus Research* vol. 100 247–278 (Elsevier, 2018).

18. Swevers, L., Liu, J. & Smagghe, G. Defense Mechanisms against Viral Infection in Drosophila: RNAi and Non-RNAi. *Viruses* **10**, 230 (2018).

19. Galiana-Arnoux, D., Dostert, C., Schneemann, A., Hoffmann, J. A. & Imler, J.-L. Essential function in vivo for Dicer-2 in host defense against RNA viruses in drosophila. *Nat. Immunol.* **7**, 590–597 (2006).

20. van Rij, R. P. *et al.* The RNA silencing endonuclease Argonaute 2 mediates specific antiviral immunity in Drosophila melanogaster. *Genes Dev.* **20**, 2985–2995 (2006).

21. Wang, X.-H. *et al.* RNA Interference Directs Innate Immunity Against Viruses in Adult Drosophila. *Science* **312**, 452–454 (2006).

22. Zambon, R. A., Vakharia, V. N. & Wu, L. P. RNAi is an antiviral immune response against a dsRNA virus in Drosophila melanogaster. *Cell. Microbiol.* **8**, 880–889 (2006).

23. Costa, A., Jan, E., Sarnow, P. & Schneider, D. The Imd Pathway Is Involved in Antiviral Immune Responses in Drosophila. *PLoS ONE* **4**, e7436 (2009).

24. Sansone, C. L. *et al.* Microbiota-Dependent Priming of Antiviral Intestinal Immunity in Drosophila. *Cell Host Microbe* **18**, 571–581 (2015).

25. Ferreira, Á. G. *et al.* The Toll-Dorsal Pathway Is Required for Resistance to Viral Oral Infection in Drosophila. *PLoS Pathog.* **10**, e1004507 (2014).

26. Zambon, R. A., Nandakumar, M., Vakharia, V. N. & Wu, L. P. The Toll pathway is important for an antiviral response in Drosophila. *Proc. Natl. Acad. Sci.* **102**, 7257–7262 (2005).

27. Dostert, C. *et al.* The Jak-STAT signaling pathway is required but not sufficient for the antiviral response of drosophila. *Nat. Immunol.* **6**, 946–953 (2005).

28. Merkling, S. H. *et al.* The Epigenetic Regulator G9a Mediates Tolerance to RNA Virus Infection in Drosophila. *PLOS Pathog.* **11**, e1004692 (2015).

29. Christian, P. D. & Johnson, K. N. The novel genome organization of the insect picorna-like virus Drosophila C virus suggests this virus belongs to a previously undescribed virus family. *J. Gen. Virol.* **79**, 191–203 (1998).

832 30. Jousset, F. X. & Plus, N. [Study of the vertical transmission and horizontal
833 transmission of 'Drosophila melanogaster' and 'Drosophila immigrans' picornavirus
834 (author's transl)]. *Ann. Microbiol. (Paris)* **126**, 231–249 (1975).
835 31. Mondotte, J. A. *et al.* Immune priming and clearance of orally acquired RNA
836 viruses in Drosophila. *Nat. Microbiol.* **3**, 1394–1403 (2018).
837 32. Torri, A., Mongelli, V., Mondotte, J. A. & Saleh, M.-C. Viral Infection and Stress
838 Affect Protein Levels of Dicer 2 and Argonaute 2 in Drosophila melanogaster. *Front.*
839 *Immunol.* **11**, 362 (2020).
840 33. Deddouche, S. *et al.* The DExD/H-box helicase Dicer-2 mediates the induction
841 of antiviral activity in drosophila. *Nat. Immunol.* **9**, 1425–1432 (2008).
842 34. Gomariz-Zilber, E., Jeune, B. & Thomas-Orillard, M. Limiting conditions of the
843 horizontal transmission of the Drosophila C virus in its host (D. melanogaster). *Acta*
844 *Oecologica* **19**, 125–137 (1998).
845 35. Stevanovic, A. L. & Johnson, K. N. Infectivity of Drosophila C virus following
846 oral delivery in Drosophila larvae. *J. Gen. Virol.* **96**, 1490–1496 (2015).
847 36. Royet, J. Epithelial homeostasis and the underlying molecular mechanisms in
848 the gut of the insect model Drosophila melanogaster. *Cell. Mol. Life Sci.* **68**, 3651–
849 3660 (2011).
850 37. Buchon, N., Broderick, N. A., Poidevin, M., Pradervand, S. & Lemaitre, B.
851 Drosophila Intestinal Response to Bacterial Infection: Activation of Host Defense and
852 Stem Cell Proliferation. *Cell Host Microbe* **5**, 200–211 (2009).
853 38. Buchon, N., Broderick, N. A., Chakrabarti, S. & Lemaitre, B. Invasive and
854 indigenous microbiota impact intestinal stem cell activity through multiple pathways in
855 Drosophila. *Genes Dev.* **23**, 2333–2344 (2009).

856 39. Buchon, N., Broderick, N. A., Kuraishi, T. & Lemaitre, B. DrosophilaEGFR
857 pathway coordinates stem cell proliferation and gut remodeling following infection.
858 *BMC Biol.* **8**, 152 (2010).
859 40. Xu, J. *et al.* ERK signaling couples nutrient status to antiviral defense in the
860 insect gut. *Proc. Natl. Acad. Sci.* **110**, 15025–15030 (2013).
861 41. Lauring, A. S. & Andino, R. Quasispecies Theory and the Behavior of RNA
862 Viruses. *PLoS Pathog.* **6**, e1001005 (2010).
863 42. Isakov, O. *et al.* Deep sequencing analysis of viral infection and evolution
864 allows rapid and detailed characterization of viral mutant spectrum. 10.
865 43. Hartl, D. L. & Clark, A. G. Principles of Population Genetics, Fourth Edition. 7.
866 44. Travisano, M., Mongold, J. A., Bennett, A. F. & Lenski, R. E. Experimental
867 Tests of the Roles of Adaptation, Chance, and History in Evolution. **267**, 5 (1995).
868 45. Desai, M. M. & Fisher, D. S. Beneficial Mutation–Selection Balance and the
869 Effect of Linkage on Positive Selection. *Genetics* **176**, 1759–1798 (2007).
870 46. Miralles, R. Clonal Interference and the Evolution of RNA Viruses. *Science*
871 **285**, 1745–1747 (1999).
872 47. Miralles, R., Moya, A. & Elena, S. F. Diminishing Returns of Population Size in
873 the Rate of RNA Virus Adaptation. *J. Virol.* **74**, 3566–3571 (2000).
874 48. Pepin, K. M. & Wichman, H. A. Experimental evolution and genome
875 sequencing reveal variation in levels of clonal interference in large populations of
876 bacteriophage ϕX174. *BMC Evol. Biol.* **8**, 85 (2008).
877 49. Navarro R, Ambrós S, Martínez F, Elena SF. 2017. Diminishing returns of
878 inoculum size on the rate of a plant RNA virus evolution. Eurphys Lett. 120:38001.
879 (2017).

880 50. Pandit, A. & de Boer, R. J. Reliable reconstruction of HIV-1 whole genome
881 haplotypes reveals clonal interference and genetic hitchhiking among immune
882 escape variants. *Retrovirology* **11**, 56 (2014).
883 51. Strelkowa, N. & Lässig, M. Clonal Interference in the Evolution of Influenza.
884 *Genetics* **192**, 671–682 (2012).
885 52. Gerrish, P. J. & Lenski, R. E. The fate of competing beneficial mutations in an
886 asexual population. in *Mutation and Evolution* (eds. Woodruff, R. C. & Thompson, J.
887 N.) vol. 7 127–144 (Springer Netherlands, 1998).
888 53. Held, T., Klemmer, D. & Lässig, M. Survival of the simplest in microbial
889 evolution. *Nat. Commun.* **10**, 2472 (2019).
890 54. Novella, I. S., Zárate, S., Metzgar, D. & Ebendick-Corpus, B. E. Positive
891 Selection of Synonymous Mutations in Vesicular Stomatitis Virus. *J. Mol. Biol.* **342**,
892 1415–1421 (2004).
893 55. Zanini, F. & Neher, R. A. Quantifying Selection against Synonymous Mutations
894 in HIV-1 env Evolution. *J. Virol.* **87**, 11843–11850 (2013).
895 56. Martínez, M. A., Jordan-Paiz, A., Franco, S. & Nevot, M. Synonymous Virus
896 Genome Recoding as a Tool to Impact Viral Fitness. *Trends Microbiol.* **24**, 134–147
897 (2016).
898 57. Kieft, J. S., Zhou, K., Jubin, R. & Doudna, J. A. Mechanism of ribosome
899 recruitment by hepatitis C IRES RNA. *RNA* **7**, 194–206 (2001).
900 58. van Rij, R. P. *et al.* The RNA silencing endonuclease Argonaute 2 mediates
901 specific antiviral immunity in Drosophila melanogaster. *Genes Dev.* **20**, 2985–2995
902 (2006).

903 59. Zhang, L. *et al.* lncRNA Sensing of a Viral Suppressor of RNAi Activates Non-
904 canonical Innate Immune Signaling in Drosophila. *Cell Host Microbe* **27**, 115-128.e8
905 (2020).
906 60. Navarro, R. *et al. Defects in plant immunity modulate the rates and patterns of*
907 *RNA virus evolution*. http://biorxiv.org/lookup/doi/10.1101/2020.10.13.337402 (2020)
908 doi:10.1101/2020.10.13.337402.
909 61. Merkling, S. H. & van Rij, R. P. Analysis of resistance and tolerance to virus
910 infection in Drosophila. *Nat. Protoc.* **10**, 1084–1097 (2015).
911 62. Lee, Y. S. *et al.* Distinct Roles for Drosophila Dicer-1 and Dicer-2 in the
912 siRNA/miRNA Silencing Pathways. *Cell* **117**, 69–81 (2004).
913 63. Okamura, K. Distinct roles for Argonaute proteins in small RNA-directed RNA
914 cleavage pathways. *Genes Dev.* **18**, 1655–1666 (2004).
915 64. Levashina, E. A., Ohresser, S., Lemaitre, B. & Imler, J. L. Two distinct
916 pathways can control expression of the gene encoding the Drosophila antimicrobial
917 peptide metchnikowin. *J. Mol. Biol.* **278**, 515–527 (1998).
918 65. Rutschmann, S. *et al.* The Rel Protein DIF Mediates the Antifungal but Not the
919 Antibacterial Host Defense in Drosophila. *Immunity* **12**, 569–580 (2000).
920 66. Hedengren, M. *et al.* Relish, a Central Factor in the Control of Humoral but Not
921 Cellular Immunity in Drosophila. *Mol. Cell* **4**, 827–837 (1999).
922 67. Díaz-Benjumea, F. J. & García-Bellido, A. Behaviour of cells mutant for an
923 EGF receptor homologue of Drosophila in genetic mosaics. *Proc. Biol. Sci.* **242**, 36–
924 44 (1990).
925 68. Reed, L. J. & Muench, H. A SIMPLE METHOD OF ESTIMATING FIFTY PER
926 CENT ENDPOINTS12. *Am. J. Epidemiol.* **27**, 493–497 (1938).

927 69. Hothorn, T., Bretz, F. & Westfall, P. Simultaneous Inference in General
928 Parametric Models. *Biom. J.* **50**, 346–363 (2008).
929 70. Weisberg S, F. J. An R Companion to Applied Regression, Third edition.
930 Sage, Thousand Oaks CA.
931 https://socialsciences.mcmaster.ca/jfox/Books/Companion/. in (2019).
932 71. Lenth. *Estimated Marginal Means, aka Least-Squares Means. R package*
933 *version 1.5.5*. (2021).
934 72. Wickham, H. *et al.* Welcome to the Tidyverse. *J. Open Source Softw.* **4**, 1686
935 (2019).
936 73. Cornman, R. S. *et al.* Population-genomic variation within RNA viruses of the
937 Western honey bee, Apis mellifera, inferred from deep sequencing. *BMC Genomics*
938 **14**, 154 (2013).
939 74. Lequime, S., Fontaine, A., Ar Gouilh, M., Moltini-Conclois, I. & Lambrechts, L.
940 Genetic Drift, Purifying Selection and Vector Genotype Shape Dengue Virus Intra-
941 host Genetic Diversity in Mosquitoes. *PLOS Genet.* **12**, e1006111 (2016).
942 75. Benjamini, Y. & Hochberg, Y. Controlling the False Discovery Rate: A Practical
943 and Powerful Approach to Multiple Testing. *J. R. Stat. Soc. Ser. B Methodol.* **57**,
944 289–300 (1995).
945 76. Myers, M. A., Satas, G. & Raphael, B. J. CALDER: Inferring Phylogenetic
946 Trees from Longitudinal Tumor Samples. *Cell Syst.* **8**, 514-522.e5 (2019).
947 77. Smith, M. A. *et al.* E-scape: interactive visualization of single-cell
948 phylogenetics and cancer evolution. *Nat. Methods* **14**, 549–550 (2017).

Tables

Table 1. Analysis of the impact of each experimental variable on the evolution of DCV nucleotide diversity (mean $\log_{10}(\pi)$ per site). The site-averaged nucleotide diversity (π) on all polymorphic sites (*n* = 1869) across the full-length viral genome was determined, the $\log_{10}$-transformed π values were fitted to the generalized linear model (GLM) and the impact of the variables determined by an Analysis of Deviance (Type III tests). BR: biological replicate; VP: viral passage; FG: fly genotype, GR: genomic region. *P ≤ 0.1, **P ≤ 0.01, ***P ≤ 0.001.

	Experimental variable	χ^2	d.f.	*p*	
Full-length DCV genome	BR	2.2528	1	0.1334	
	VP	1.6460	1	0.1995	
	FG	25.5447	8	0.0013	**
	(BR) × VP	0.0024	1	0.9606	
	(BR) × FG	14.2963	8	0.0744	
	VP × FG	12.1679	8	0.1439	
	(BR) × VP × FG	10.4253	8	0.2364	
Each DCV genomic region	BR	1.2107	1	0.2712	
	VP	2.3528	1	0.1251	
	FG	27.1779	8	0.0007	***
	GR	11.6982	3	0.0085	**
	(BR) × VP	0.0001	1	0.9931	
	(BR) × FG	16.3143	8	0.0381	*
	VP × FG	8.3498	8	0.4000	
	(BR) × GR	0.7452	3	0.8625	
	VP × GR	0.9130	3	0.8223	
	FG × GR	24.0586	24	0.4583	
	(BR) × VP × FG	12.8802	8	0.1160	
	(BR) × VP × GR	0.1274	3	0.9884	
	(BR) × FG × GR	24.4811	24	0.4344	
	VP × FG × GR	10.5776	24	0.9917	
	(BR) × VP × FG × GR	28.3112	24	0.2471	

Table 2. Mutations for which significant estimates of fitness effects have been obtained. For each mutation, we indicate whether it already existed in the S2 DCV stock (and at which frequency) or arose during the evolution experiment. We also provide the estimated selection coefficient, its SEM and statistical significance. Cases significant after FDR correction are marked with an asterisk.

Fly genotype	Biol. Rep.	Mutation	Standing variation (frequency)	Selection coefficient per passage (± SEM)	*P*
w^{1118}	1	VP2/G6311C R16P	Yes (0.0104)	1.2039 ±0.2543	0.0418
w^{1118}	2	VP3/U7824C	Yes (0.1457)	0.4780 ±0.0617	< 0.0001*
$Dcr\text{-}2^{L811fsX/L811fsX}$	1	-			
$Dcr\text{-}2^{L811fsX/L811fsX}$	2	RpRd/U5302C	No	0.3877 ±0.0973	0.0073
		VP1/C8227U H655Y	Yes (0.0147)	0.3735 ±0.1368	0.0258
		VP1/C8424U	Yes (0.0139)	0.3880 ±0.1407	0.0248
$Dcr\text{-}2^{R416X/R416X}$	1	VP2/C6932U A223V	Yes (0.0084)	0.2135 ±0.0169	< 0.0001*
$Dcr\text{-}2^{R416X/R416X}$	2	VP2/G6379A A39T	Yes (0.0098)	0.2074 ±0.0555	0.0057
		VP3/A7465G I401V	Yes (0.0088)	0.1185 ±0.0338	0.0100
		VP3/U7824C	Yes (0.1457)	–0.2887 ±0.0884	0.0309
$Ago\text{-}2^{414/414}$	1	-			
$Ago\text{-}2^{414/414}$	2	5'UTR/A280U	Yes (0.1176)	–0.1307 ±0.0376	0.0084
		VP3/U7824C	Yes (0.1457)	0.5251 ±0.1050	0.0024
		VP1/C8227U H655Y	Yes (0.0147)	0.6238 ±0.1077	0.0007
		VP1/C8424U	Yes (0.0139)	0.6206 ±0.1252	0.0026
$Spz^{2/2}$	1	5'UTR/A280U	Yes (0.1176)	–0.2092 ±0.0735	0.0215
		VP2/G6931A A223T	No	0.5420 ±0.1477	0.0105
$Spz^{2/2}$	2	2A/A1128C D110A	Yes (0.0041)	–0.0229 ±0.0065	0.0246
		3C-Prot/A3787G	No	0.5238 ±0.0757	0.0002*
		3C-Prot/G4394A V1199I	No	0.5982 ±0.0764	0.0002*
		VP1/G8536A V758I	No	0.7038 ±0.0915	0.0006*
		IGR/A6108G	Yes (0.0044)	0.4873 ±0.0692	0.0002*
		VP3/G8090A R609H	Yes (0.0200)	0.4947 ±0.0722	0.0001*
$Dif^{1/1}$	1	VP3/A7465G I401V	Yes (0.0088)	0.3213 ±0.1173	0.0338
		VP3/G7956A	No	0.2000 ±0.0335	0.0094
$Dif^{1/1}$	2	5'UTR/A280U	Yes (0.1176)	0.5157 ±0.1289	0.0052
		VP1/U8629C S5058P	Yes (0.0898)	0.4864 ±0.1175	0.0043
$Rel^{E20/E20}$	1	5'UTR/A280U	Yes (0.1176)	0.3430 ±0.1017	0.0097
		RdRp/A5404G	Yes (0.0929)	0.3993 ±0.1217	0.0135
		VP2/U6303A N13K	Yes (0.0037)	0.5724 ±0.1409	0.0036
		VP3/U7824C	Yes (0.1457)	–0.2804 ±0.0206	0.0467
$Rel^{E20/E20}$	2	5'UTR/A280U	Yes (0.1176)	–0.0917 ±0.0277	0.0130
		2B/C1412U	Yes (0.1301)	0.4554 ±0.0119	0.0166
		VP3/C7760A T499N	No	0.1340 ±0.0195	0.0005
$Vago^{\Delta M10/\Delta M10}$	1	2B/C1412U	Yes (0.1301)	0.2386 ±0.0549	0.0025
		3C-Prot/A3703G	No	0.2859 ±0.0537	0.0031
		RdRp/U5188A	Yes (0.1325)	0.2869 ±0.0705	0.0268
		VP2/C6932U A223V	Yes (0.0084)	0.1368 ±0.0553	0.0426
		VP1/C8227U H655Y	Yes (0.0147)	0.1936 ±0.0291	0.0002*
		VP1/C8424U	Yes (0.0139)	0.1915 ±0.0283	0.0001*
		VP1/U8697C	No	0.2053 ±0.0325	0.0002*
		3'UTR/U9163A	No	0.1473 ±0.0622	0.0497
$Vago^{\Delta M10/\Delta M10}$	2	2C-Hel/G1756A	Yes (0.0059)	0.3467 ±0.1293	0.0364
		VP2/A6300U E12D	No	0.3681 ±0.1297	0.0470
		VP3/U7824C	Yes (0.1372)	0.1517 ±0.0391	0.0060
$Egfr^{1/1}$	1	5'UTR/A280U	Yes (0.1176)	0.1394 ±0.0364	0.0050
		3C-Prot/U3643A	No	–0.2064 ±0.0592	0.0399
		VP1/A8201G Q646R	Yes (0.0045)	0.3198 ±0.0736	0.0225
		VP2/A6660U	No	–0.1906 ±0.0641	0.0409
		VP2/G6868A V8162I	No	0.3302 ±0.0389	0.0001
		VP3/A7465G I401V	Yes (0.0088)	–0.1053 ±0.0359	0.0261
		VP3/U7824C	Yes (0.1457)	0.0997 ±0.0410	0.0411
$Egfr^{1/1}$	2	5'UTR/A198G	No	0.1035 ±0.0363	0.0246
		RdRp/U4810C	Yes (0.1152)	–0.2635 ±0.0301	0.0128
		RdRp/C5713U	Yes (0.1148)	–0.3036 ±0.0276	0.0082
		VP2/G6379A A39T	Yes (0.0082)	0.0630 ±0.0254	0.0381
		VP3/U7824C	Yes (0.1457)	–0.1090 ±0.0402	0.0421
		VP3/G8090A R609H	Yes (0.0200)	0.0764 ±0.0289	0.0333
		VP1/U8250G H662Q	Yes (0.0201)	0.1734 ±0.0326	0.0060

962 **Figures**

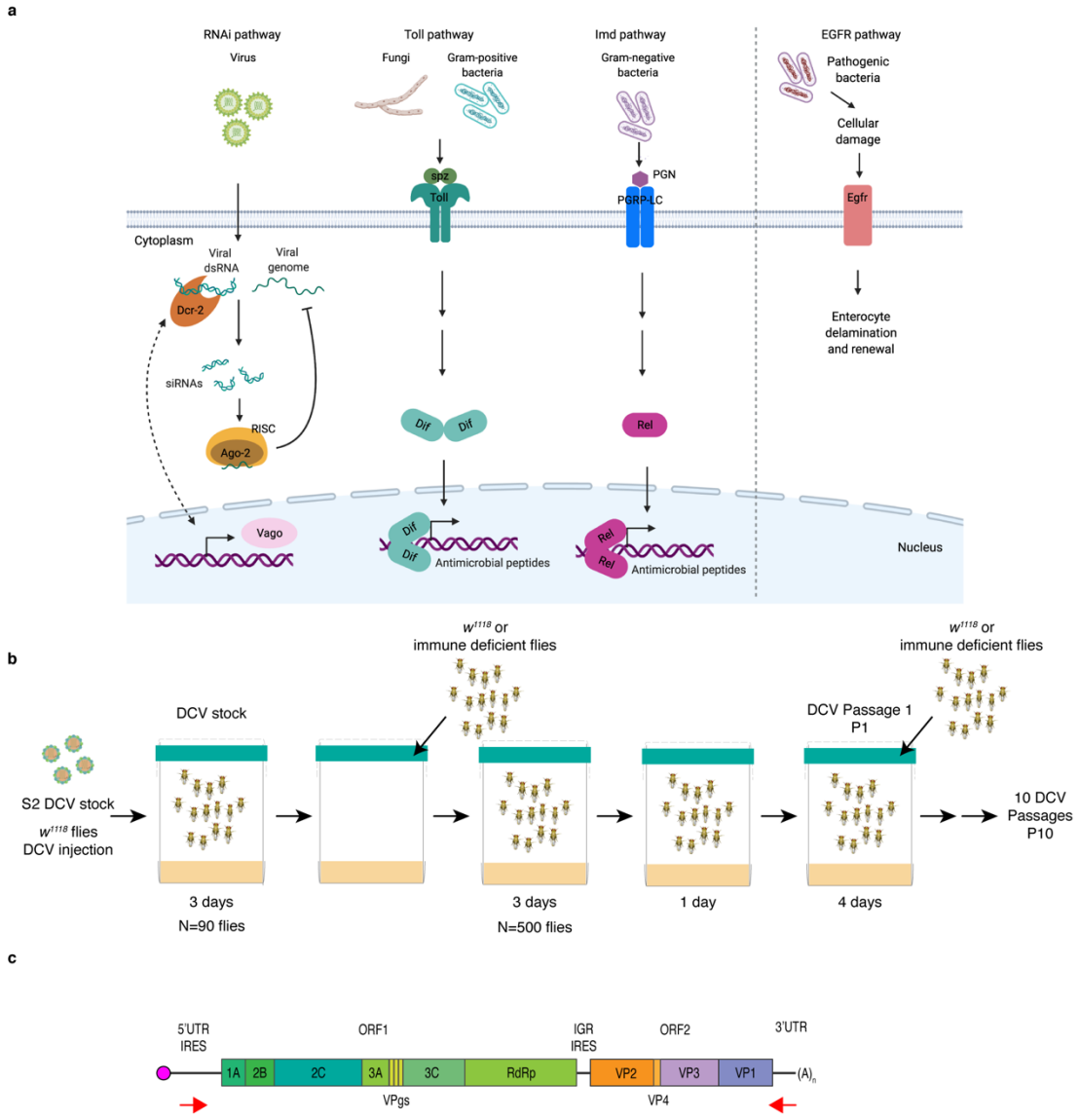

963 **Figure 1. Experimental design. a)** Simplified scheme of *D. melanogaster* immune
964 pathways. The siRNA pathway is triggered by virus-derived dsRNA, recognized by
965 Dcr-2 and cleaved into viral siRNAs, which guide the recognition and cleavage of
966 viral RNA by Ago-2 controlling virus infection. The Toll pathway is activated when spz
967 binds to the Toll receptor, leading to the activation of NF-κB transcription factors (e.g.
968 Dif). The Imd pathway is triggered after the recognition of microbial peptidoglycans
969 (PGN) by PGRP-LC, ultimately leading to the activation of Rel. Toll and Imd

pathways induce the expression of antimicrobial peptides to control infection. The expression of Vago is induced after infection with DCV. The EGFR pathway is triggered in the gut after bacterial damage and leads to delamination of enterocytes and renewal. Created with BioRender.com. **b)** Scheme of the DCV evolution experiment. To produce the DCV stock, w^{1118} female flies were injected with DCV from a stock produced in S2 Drosophila cells (S2 DCV stock), placed in cages containing fresh Drosophila medium, left for 3 days and then removed to place in these DCV contaminated cages $N = 500$ w^{1118} or immune deficient males and females. Flies were feed *ad libitum* for 3 days, moved to a clean cage for 1 day, and further placed into a new clean cage for 4 days, when they were harvested (DCV passage 1, P1). A new group of 500 flies was placed in contaminated cages. This procedure was repeated 10 times (10 DCV passages, P1 to P10) and replicated twice (biological replicates BR1 and BR2). For each passage and fly genotype, high-throughput sequencing and viral stocks for phenotypic characterization were obtained. **c)** Scheme of DCV genome and the location of primers used to amplify the genome. The viral genome is composed of single-stranded positive-sense RNA and contains two ORFs. ORF 1 encodes for the non-structural viral proteins, 1A: viral silencing suppressor, 2C: RNA helicase, VPg: viral genome-linked protein, 3C: protease, RdRp: RNA-dependent RNA polymerase, 2B and 3A: assembly of the viral replication complex. ORF 2 encodes for DCV structural proteins VP1 to VP4 which constitute the viral capsid.

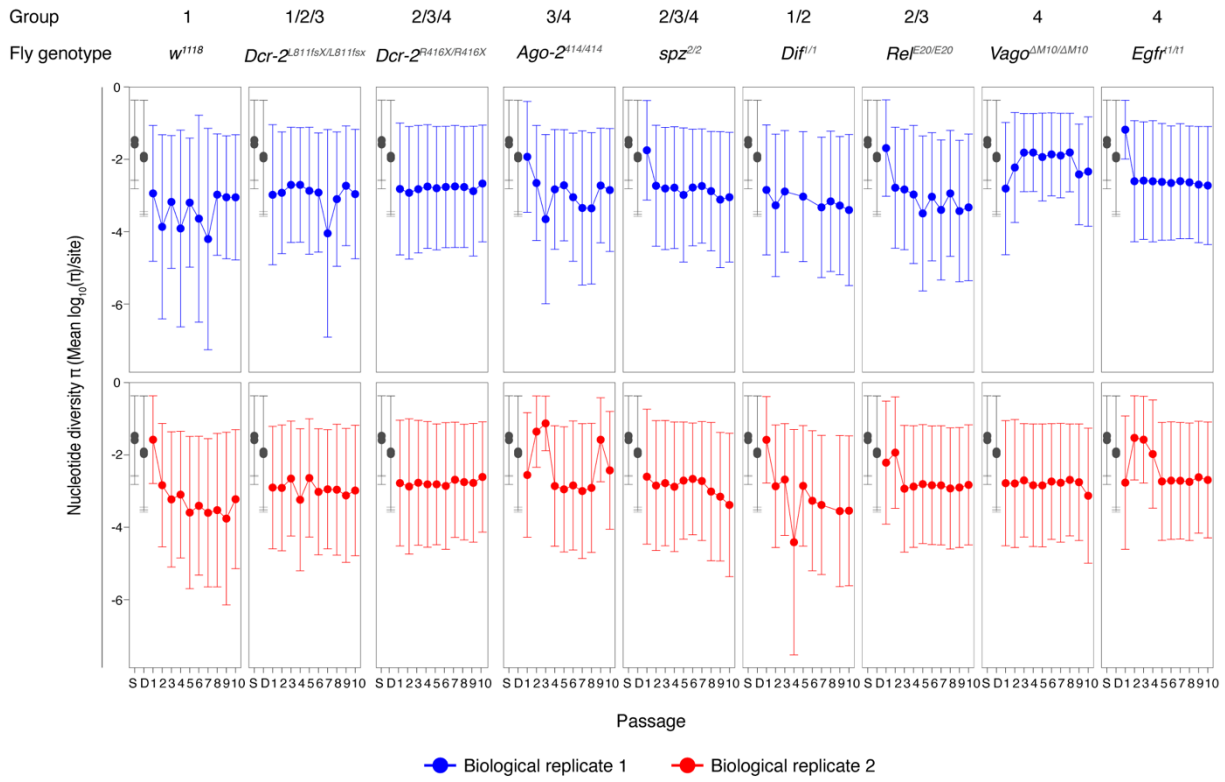

Figure 2. Viral nucleotide diversity differently evolves in each host genotype. Trajectory of the site-averaged nucleotide diversity (π) on all polymorphic sites (*n* = 1869) across the full-length DCV genome found for each fly genotype and in each biological replicate of the evolution experiment. Group: DCV population diversity found in each fly genotype was pairwise compared and grouped by similarity after a Bonferroni *post hoc* test (Table 1 and Supplementary Table 1). S: S2 DCV stock and D: DCV stock, in grey.

998 **Figure 3. Trajectories of DCV variants across passages.** Muller plots illustrating
999 the dynamics of SNPs' frequencies along evolutionary time. Each color represents
1000 the dynamics of a different SNP.

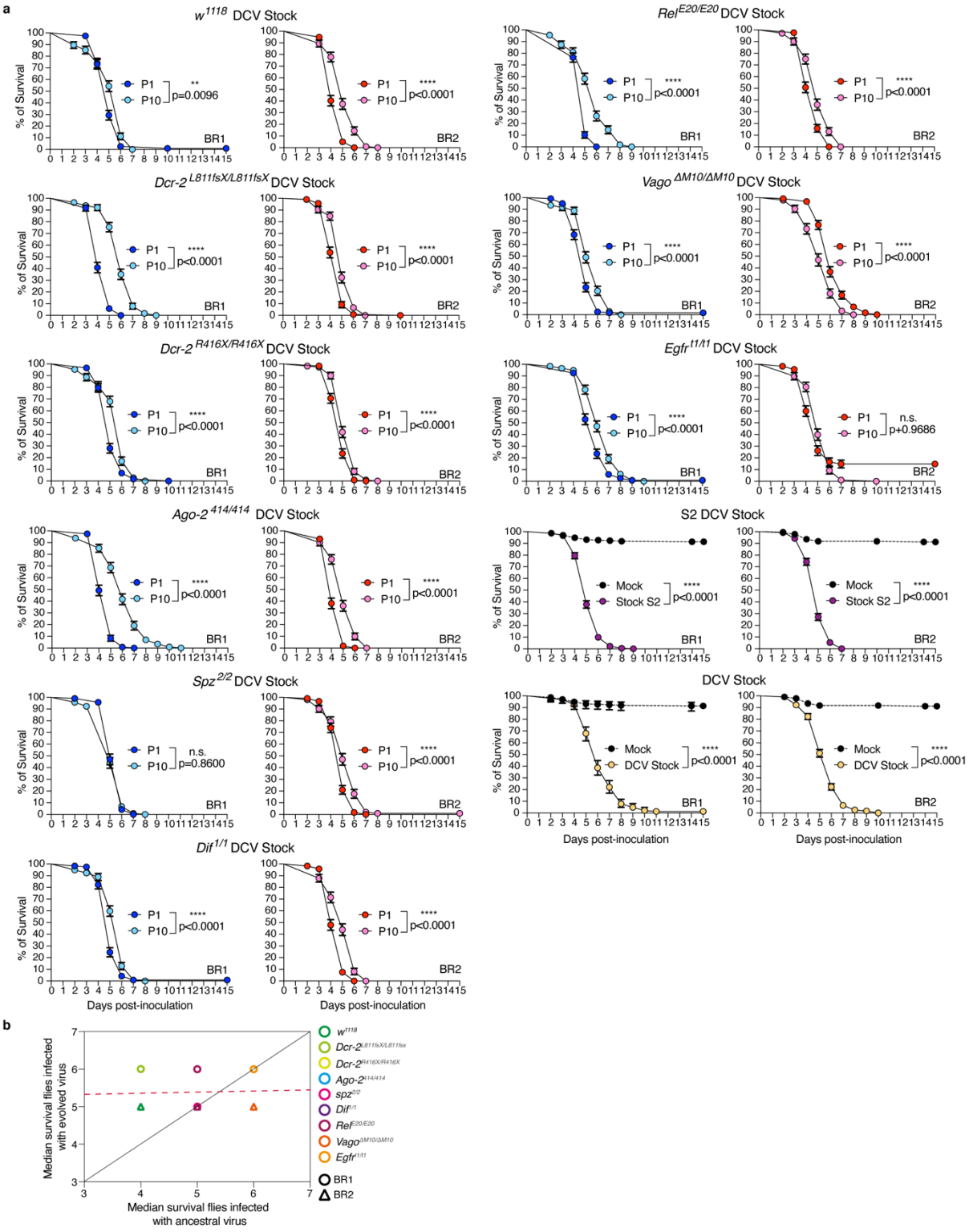

1001 **Figure 4. DCV virulence decreases in the absence of immune pathways.** DCV
1002 infectious stocks were prepared from viral passages P1 and P10 and from each fly
1003 genotype. *w*^{1118} flies were intrathoracically inoculated with 10 $TCID_{50}$ units of each
1004 DCV stock and survival of the flies was measured daily. **a)** Survival curves shown in

1005 the figure are the combination of the two independent replicates, with three technical
1006 replicates each, of a total of at least $N = 98$ flies per treatment. Error bars indicate ±
1007 Standard error of the mean (SEM); n.s., not significant. Survival curves were
1008 compared via log-rank (Mantel–Cox) tests. **b)** Test of the contribution of historical
1009 contingency evolved (P10) *vs* ancestral (P1) DCV virulence. The dashed red line
1010 represents the linear regression, and the black line represents the expected
1011 relationship under the null hypothesis of ancestral differences in DCV virulence which
1012 are maintained after evolution despite noise introduced by random events (mutation
1013 and drift).

Extended Data

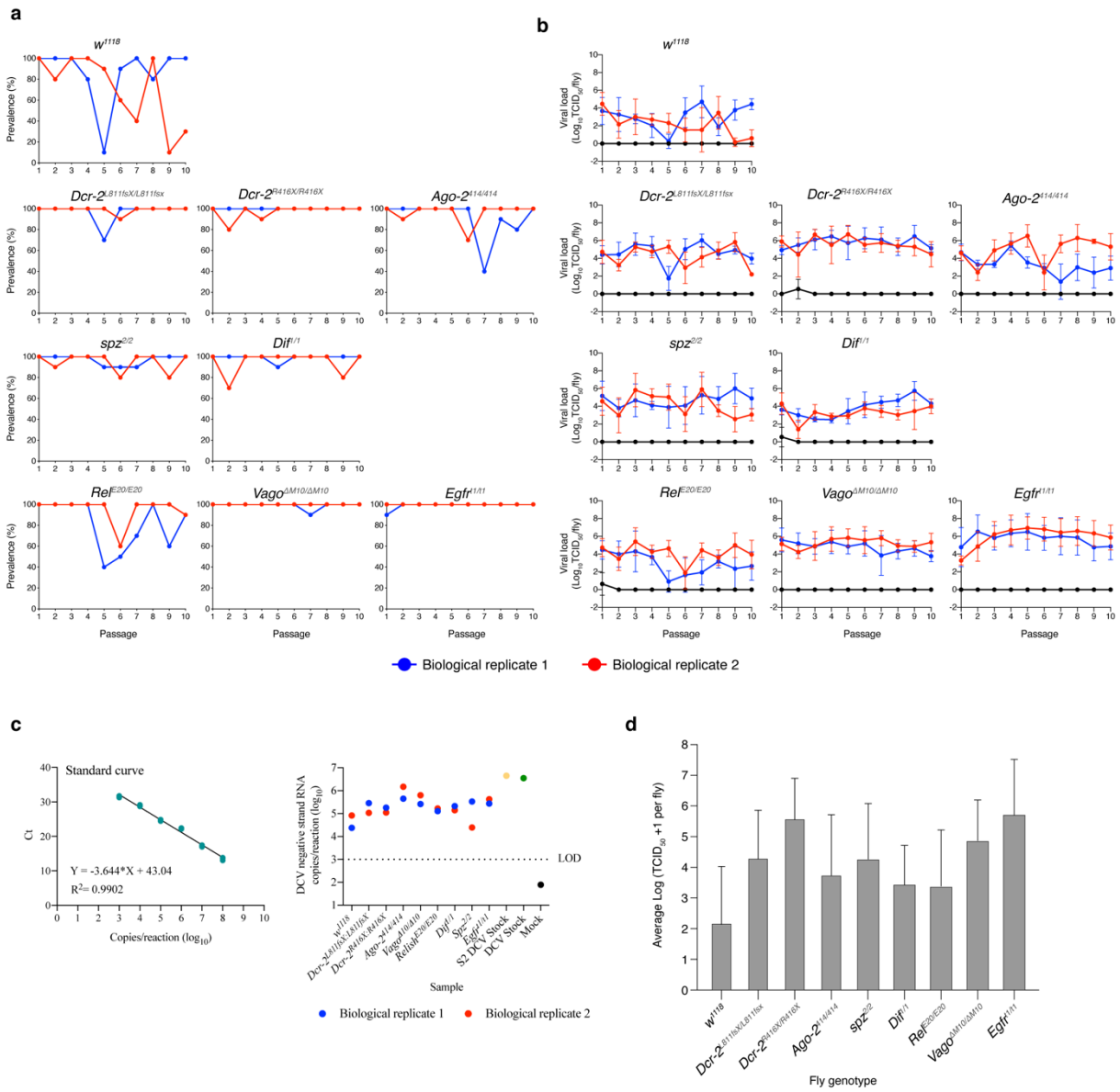

1015 **Extended Data Figure 1. Viral load and prevalence across the DCV evolution**
1016 **experiment.** Viral load of 10 individual flies coming from DCV inoculated cages and
1017 four individual flies coming from mock inoculated cages was determined by $TCID_{50}$.
1018 **a)** Prevalence, calculated as the percentage of flies positive by $TCID_{50}$. **b)** Viral load
1019 determined by $TCID_{50}$ in each genotype across the 10 DCV passages. **c)** DCV
1020 replication assessed by negative strand RT-qPCR. Left panel: standard curve
1021 produced from a tenfold dilution series over a range from 10^8 to 10^3 copies per
1022 reaction of in vitro transcribed RNA corresponding to a portion of the full-length

negative strand DCV RNA (slope = -3.644, R^2 = 0.990, efficiency = 88.25%). Right panel: amount of negative strand DCV RNA present in the viral stocks produced from each fly genotype in P10, S2 DCV stock and DCV stock. Mock infected flies were added as controls. LOD: Limit of detection of DCV negative stranded RNA. **d)** Average viral loads per individual fly of each genotype estimated from the GLM fitted to the data shown in panel b. Error bars represent ±1 SD.

	Condition	mean log_{10} (π) per site	SE	d.f.	asymp.LCL	asymp.UCL	Group
Full length genome, all viral passages	*w*^{1118}	0.0005	0.0001	Inf	0.0003	0.0009	1
	Dif$^{1/1}$	0.0007	0.0002	Inf	0.0004	0.0013	12
	Dcr-2$^{L811fsX/L811fsX}$	0.0011	0.0002	Inf	0.0006	0.0019	123
	Rel$^{E20/20}$	0.0014	0.0003	Inf	0.0008	0.0025	23
	spz$^{2/2}$	0.0015	0.0003	Inf	0.0009	0.0027	234
	Dcr-2$^{R416X/R416X}$	0.0017	0.0003	Inf	0.0009	0.0029	234
	Ago-2$^{414/414}$	0.0023	0.0005	Inf	0.0013	0.0041	34
	Egfr$^{1/1}$	0.0036	0.0007	Inf	0.0020	0.0063	4
	Vago$^{DM10/DM10}$	0.0036	0.0007	Inf	0.0021	0.0063	4
All fly genotype, all viral passages	3'UTR	$1.98{\cdot}10^{-05}$	$2.44{\cdot}10^{-06}$	Inf	$1.46{\cdot}10^{-05}$	$2.70{\cdot}10^{-05}$	1
	5'UTR IRES	0.0001	$1.25{\cdot}10^{-05}$	Inf	0.0001	0.0002	2
	ORF1	0.0004	$3.68{\cdot}10^{-05}$	Inf	0.0004	0.0005	3
	ORF2	0.0006	$4.91{\cdot}10^{-05}$	Inf	0.0005	0.0007	3
Full length DCV genome, P5	*w*^{1118}	0.0004	0.0002	10	0.0001	0.0023	12
	Rel$^{E20/20}$	0.0007	0.0003	10	0.0001	0.0040	12
	Dif$^{1/1}$	0.0011	0.0005	10	0.0002	0.0064	12
	spz$^{2/2}$	0.0014	0.0007	10	0.0003	0.0080	12
	Ago-2$^{414/414}$	0.0015	0.0007	10	0.0003	0.0082	12
	Dcr-2$^{R416X/R416X}$	0.0016	0.0007	10	0.0003	0.0088	12
	Dcr-2$^{L811fsX/L811fsX}$	0.0018	0.0008	10	0.0003	0.0099	12
	Egfr$^{1/1}$	0.0021	0.0010	10	0.0004	0.0117	12
	Vago$^{DM10/DM10}$	0.0041	0.0019	10	0.0007	0.0228	12
	DCV stock R1	0.0120	0.0057	10	0.0022	0.0667	2
	DCV stock R2	0.0110	0.0052	10	0.0020	0.0612	2
Full length DCV genome, P10	*Dif*$^{1/1}$	0.0003	0.0001	10	0.0001	0.0015	1
	spz$^{2/2}$	0.0006	0.0002	10	0.0001	0.0026	1
	w^{1118}	0.0007	0.0003	10	0.0002	0.0032	1
	Rel$^{E20/20}$	0.0008	0.0003	10	0.0002	0.0036	12
	Dcr-2$^{L811fsX/L811fsX}$	0.0011	0.0004	10	0.0003	0.0046	123
	Vago$^{DM10/DM10}$	0.0019	0.0007	10	0.0004	0.0080	123
	Egfr$^{1/1}$	0.0020	0.0008	10	0.0005	0.0085	123
	Dcr-2$^{R416X/R416X}$	0.0023	0.0009	10	0.0005	0.0099	123
	Ago-2$^{414/414}$	0.0023	0.0009	10	0.0005	0.0099	123
	DCV stock R2	0.0110	0.0044	10	0.0026	0.0472	23
	DCV stock R1	0.0120	0.0048	10	0.0028	0.0514	3

Extended Data Figure 2. Grouping of DCV population swarms by similarity and increasing nucleotide diversity (π). Viral nucleotide diversity (π) was determined in each condition and grouped using a *post hoc* Bonferroni test based on the pairwise comparisons from Supplementary Table 1. SE: standard error. asymp.LCL: asymptomatic lower confidence level; asymp.UCL: asymptomatic upper confidence level.

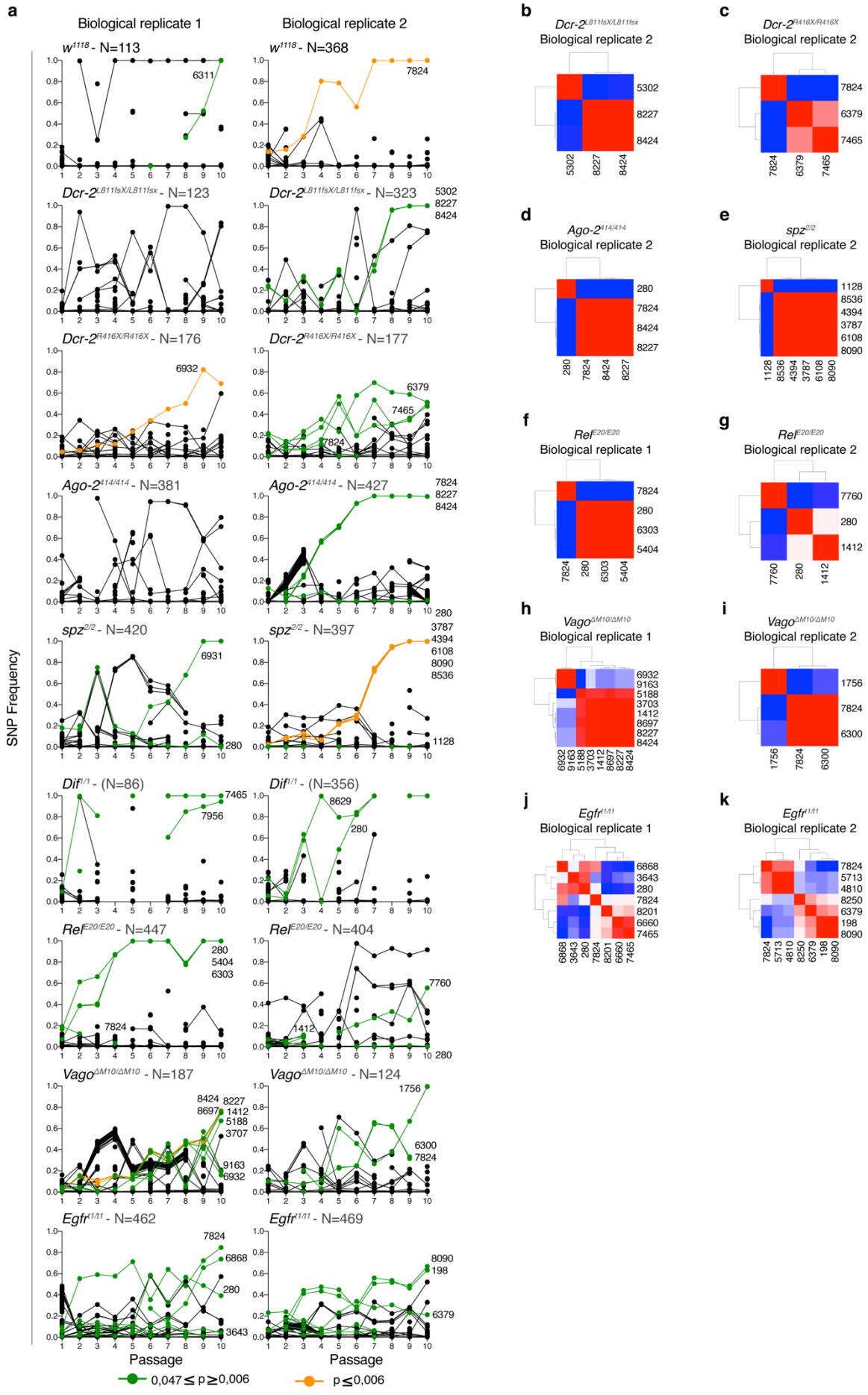
a
Biological replicate 1
Biological replicate 2
w1118 - N=113
w1118 - N=368
Dcr-2L811fsX/L811fsx - N=123
Dcr-2L811fsX/L811fsx - N=323
Dcr-2R416X/R416X - N=176
Dcr-2R416X/R416X - N=177
Ago-2414/414 - N=381
Ago-2414/414 - N=427
spz2/2 - N=420
spz2/2 - N=397
Dif1/1 - (N=86)
Dif1/1 - (N=356)
RelE20/E20 - N=447
RelE20/E20 - N=404
VagoΔM10/ΔM10 - N=187
VagoΔM10/ΔM10 - N=124
Egfr1/1 - N=462
Egfr1/1 - N=469
SNP Frequency
Passage
Passage
0,047 ≤ p ≥0,006
p ≤0,006
b
Dcr-2L811fsX/L811fsx
Biological replicate 2
c
Dcr-2R416X/R416X
Biological replicate 2
d
Ago-2414/414
Biological replicate 2
e
spz2/2
Biological replicate 2
f
RelE20/E20
Biological replicate 1
g
RelE20/E20
Biological replicate 2
h
VagoΔM10/ΔM10
Biological replicate 1
i
VagoΔM10/ΔM10
Biological replicate 2
j
Egfr1/1
Biological replicate 1
k
Egfr1/1
Biological replicate 2

Extended Data Figure 3. Evolution of DCV variants. a) Trajectories of DCV variants across passages, *N*: total number of SPNs found above the estimated frequency threshold (≥ 0.0028). Trajectories of viral variants found significant after FDR correction are show in green ($p \leq 0.006$) and yellow ($0{,}047 \leq p \leq 0.006$) (based on data from Table 2). **b)** to **k)** Heatmaps showing the Pearson correlation coefficients between mutations' frequencies along evolutionary time, ranging from blue, where no linkage between the SNPs was found, to red, where the SNPs were linked in a same viral haplotype.

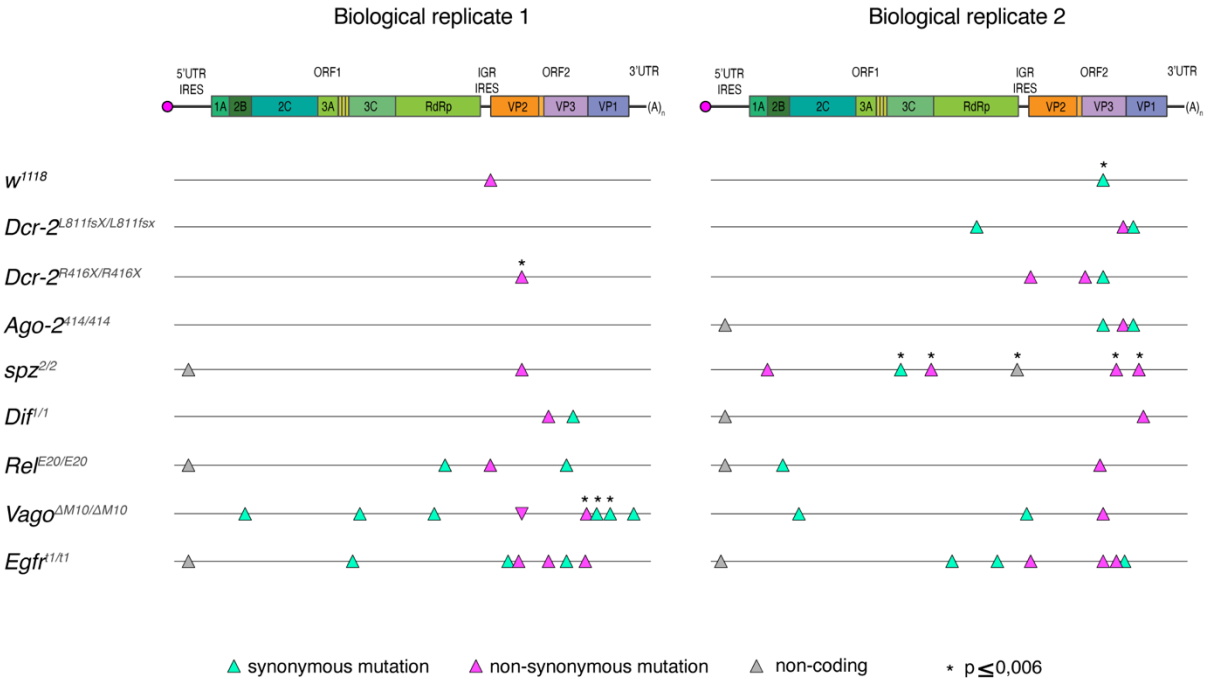

Extended Data Figure 4. SNPs on the DCV genome with significant estimates of fitness effects. Green triangles represent synonymous mutations, pink triangles nonsynonymous mutations and gray triangles mutations in non-coding sequences. Cases significant after FDR correction ($p \leq 0.006$) are marked with an asterisk (based on data from Table 2).

Supplementary Information

a

DCV

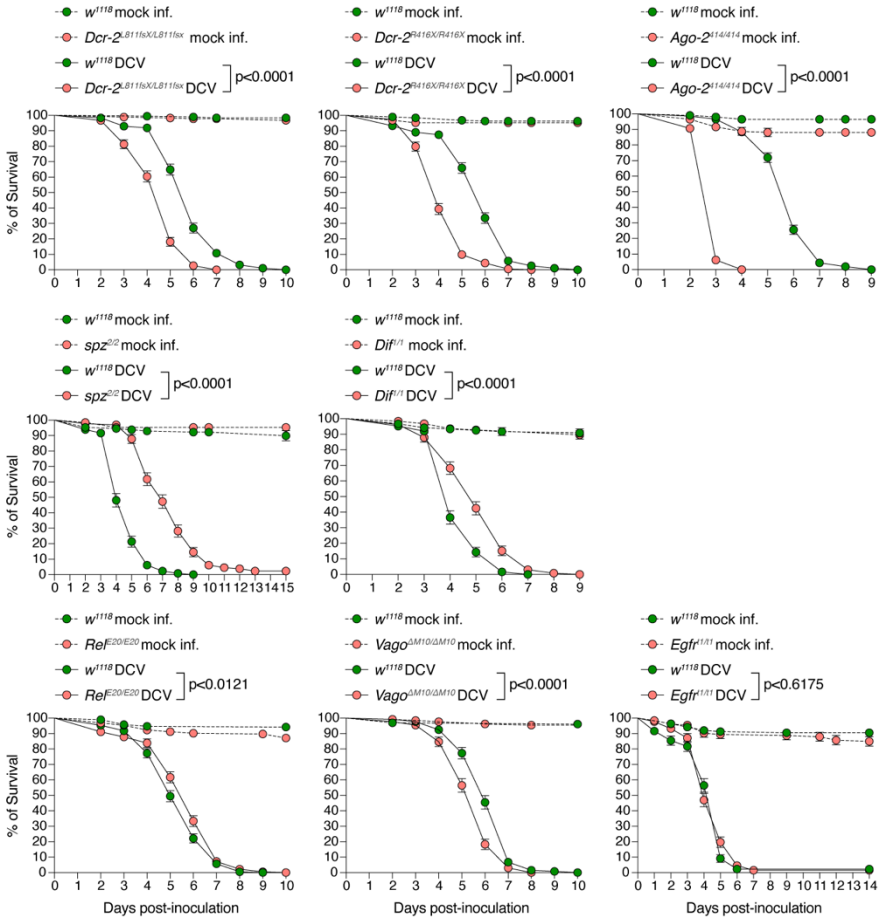

b

Enterococcus faecalis - Gram-positive

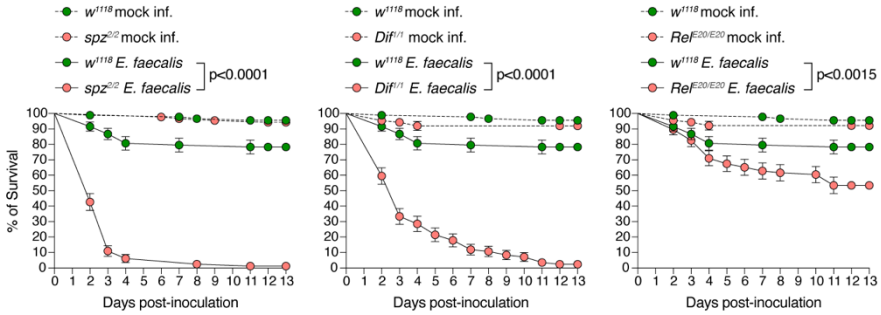

c

Erwinia carotovora - Gram-negative

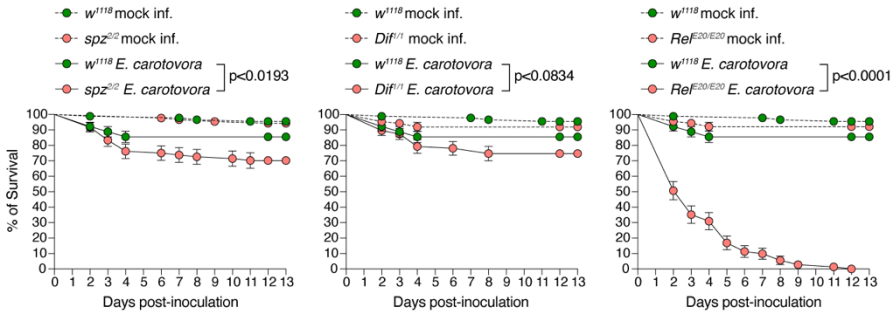

Supplementary Figure 1. Characterization of the newly produced innate immune backcrossed fly lines. Innate immune deficient fly lines backcrossed to w^{1118} genetic background were intrathoracically injected with **a)** 10 $TCID_{50}$ units of DCV, **b)** 50 nl of a suspension of optical density (OD) = 10 from *E. faecalis* (Gram + bacteria), and c) 50 nl of a suspension of OD = 200 from *E. carotovora carotovora 15* (Ecc15) (Gram + bacteria). After DCV and *E. faecalis* inoculation flies were kept at 25 °C and at 29 °C after Ecc15 inoculation. Survival was measured daily. Two independent experiments with three biological replicates of $N = 20$ flies each per condition were analyzed. Error bars indicate ±1 SEM; n.s., not significant. Survival curves were compared via log-rank (Mantel–Cox) tests.

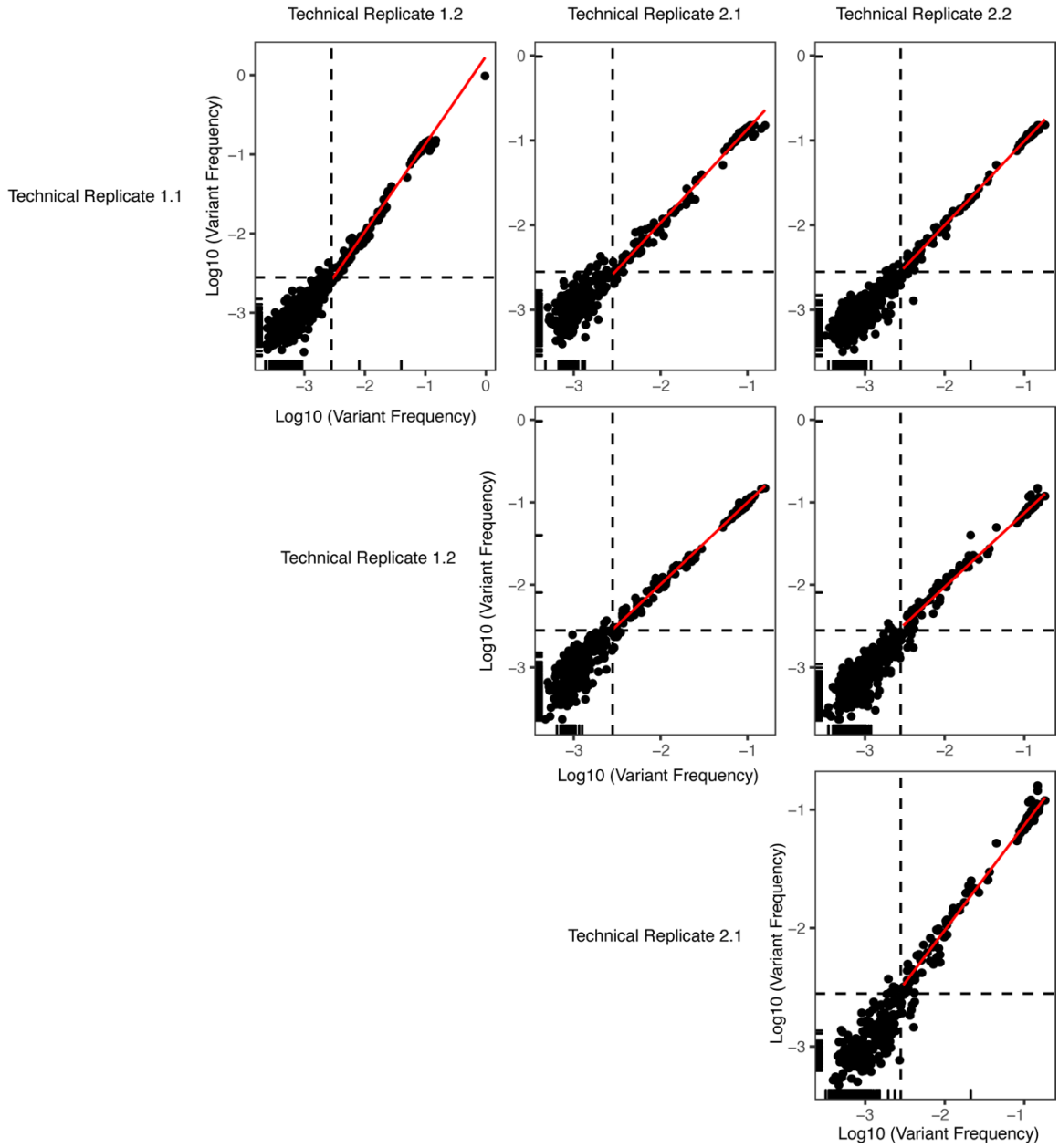

Supplementary Figure 2. Determination of NGS threshold error and mapping of sequenced derived from DCV starting stocks used. Pairwise correlation between variant frequency (log_{10}-transformed) in four technical sequencing replicates derived from S2 DCV stock. Dashed line represents the frequency threshold value used for subsequent analyses (0.0028). Red line represents the linear regression for variant frequency above the frequency threshold. Black ticks on axis represent missing variants in the other technical replicate under consideration.

Supplementary Figure 4

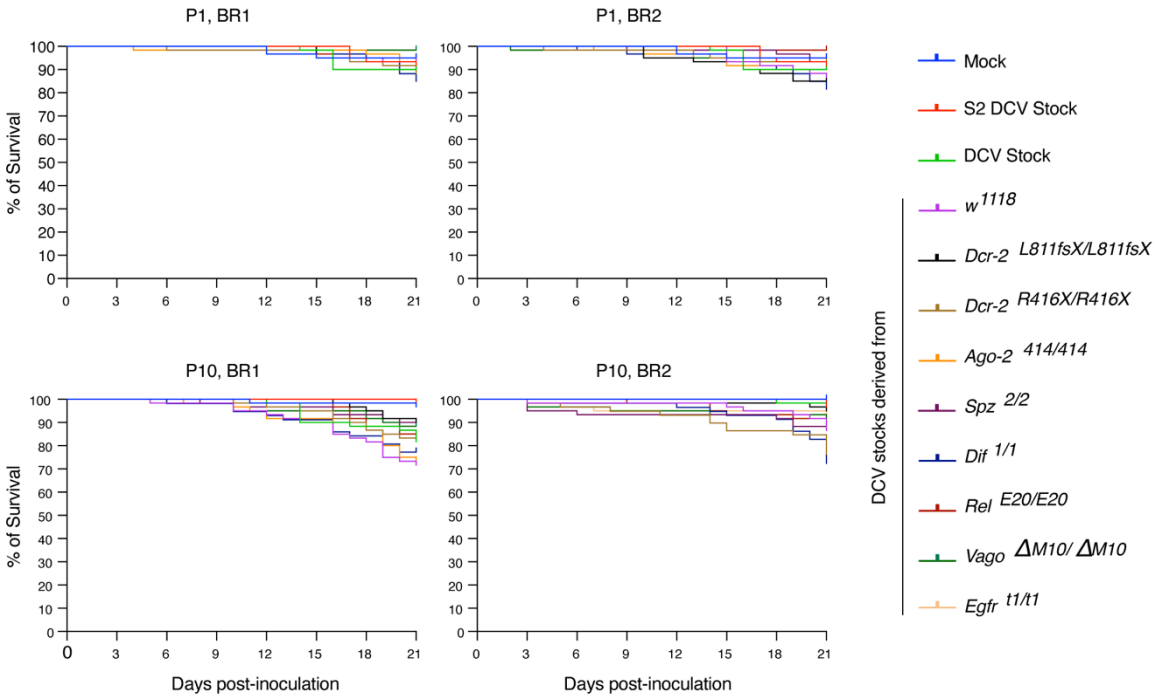

Supplementary Figure 3. Study of DCV virulence in P1 and P10 by oral infection. DCV infectious stocks were produced from viral passages P1 and P10 and from each fly genotype and biological replicate (BR1 and BR2). w^{1118} flies were orally infected with 10^6 $TCID_{50}$ units of DCV and survival was measured daily. Survival curves are the combination of two independent replicates, with three technical replicates each, of a total of at least $N = 98$ flies per treatment. Survival curves were compared via log-rank (Mantel–Cox) tests and no significant difference was found between the treatments.

Supplementary Table 1. Pairwise comparisons of DCV population diversity (Mean Log10 (π) per site). Pairwise comparison of viral nucleotide diversity between different conditions. For DCV stock, a total of four technical replicates were prepared and sequenced by pairs in 2 independent runs. For the purpose of this analysis each technical replicate derived from the same run was pooled, DCV stock R1 and R2 respectively. Statically significant p-values ($p < 0.05$) are in bold.

	Conditions compared	Estimate	SE	d.f.	*z.ratio*	*p*
Full length viral genome, all viral passages	*w*^{1118} - *Dcr-2*$^{L811fsX/L811fsX}$	0.3267	0.124	Inf	2.635	0.3026
	w^{1118} - *Dcr-2*$^{R416X/R416X}$	0.5088	0.124	Inf	4.103	**0.0015**
	w^{1118} - *Ago-2*$^{414/414}$	0.6573	0.124	Inf	5.301	**<0.0001**
	w^{1118} - *spz*$^{2/2}$	0.4750	0.124	Inf	3.831	**0.0046**
	w^{1118} - *Dif*$^{1/1}$	0.1372	0.130	Inf	1.059	1.0000
	w^{1118} - *Rel*$^{E20/20}$	0.4432	0.124	Inf	3.575	**0.0126**
	w^{1118} - *Vago*$^{DM10/DM10}$	0.8449	0.124	Inf	6.814	**<0.0001**
	w^{1118} - *Egfr*$^{t1/t1}$	0.8443	0.124	Inf	6.810	**<0.0001**
	Dcr-2$^{L811fsX/L811fsX}$ - *Dcr-2*$^{R416X/R416X}$	0.1820	0.124	Inf	1.468	1.0000
	Dcr-2$^{L811fsX/L811fsX}$ - *Ago-2*$^{414/414}$	0.3306	0.124	Inf	2.666	0.2762
	Dcr-2$^{L811fsX/L811fsX}$ - *spz*$^{2/2}$	-0.1483	0.124	Inf	-1.196	1.0000
	Dcr-2$^{L811fsX/L811fsX}$ - *Dif*$^{1/1}$	0.1895	0.130	Inf	1.462	1.0000
	Dcr-2$^{L811fsX/L811fsX}$ - *Rel*$^{E20/20}$	-0.1165	0.124	Inf	-0.939	1.0000
	Dcr-2$^{L811fsX/L811fsX}$ - *Vago*$^{DM10/DM10}$	-0.5181	0.124	Inf	-4.179	**0.0011**
	Dcr-2$^{L811fsX/L811fsX}$ - *Egfr*$^{t1/t1}$	-0.5175	0.124	Inf	-4.174	**0.0011**
	Dcr-2$^{R416X/R416X}$ - *Ago-2*$^{414/414}$	0.1485	0.124	Inf	1.198	1.0000
	Dcr-2$^{R416X/R416X}$ - *spz*$^{2/2}$	0.0337	0.124	Inf	0.272	1.0000
	Dcr-2$^{R416X/R416X}$ - *Dif*$^{1/1}$	0.3715	0.130	Inf	2.866	0.1497
	Dcr-2$^{R416X/R416X}$ - *Rel*$^{E20/20}$	0.0656	0.124	Inf	0.529	1.0000
	Dcr-2$^{R416X/R416X}$ - *Vago*$^{DM10/DM10}$	-0.3361	0.124	Inf	-2.711	0.2415
	Dcr-2$^{R416X/R416X}$ - *Egfr*$^{t1/t1}$	-0.3355	0.124	Inf	-2.706	0.2451
	Ago-2$^{414/414}$ - *spz*$^{2/2}$	0.1823	0.124	Inf	1.470	1.0000
	Ago-2$^{414/414}$ - *Dif*$^{1/1}$	0.5200	0.130	Inf	4.012	0.0022
	Ago-2$^{414/414}$ - *Rel*$^{E20/20}$	0.2141	0.124	Inf	1.727	1.0000
	Ago-2$^{414/414}$ - *Vago*$^{DM10/DM10}$	-0.1876	0.124	Inf	-1.513	1.0000
	Ago-2$^{414/414}$ - *Egfr*$^{t1/t1}$	-0.1870	0.124	Inf	-1.508	1.0000
	spz$^{2/2}$ - *Dif*$^{1/1}$	-0.3378	0.130	Inf	-2.606	0.3302
	spz$^{2/2}$ - *Rel*$^{E20/20}$	-0.0318	0.124	Inf	-0.257	1.0000
	spz$^{2/2}$ - *Vago*$^{DM10/DM10}$	-0.3699	0.124	Inf	-2.983	0.1027
	spz$^{2/2}$ - *Egfr*$^{t1/t1}$	0.3693	0.124	Inf	2.978	0.1043

	Dif$^{1/1}$ - *Rel*$^{E20/20}$	-0.3059	0.130	Inf	-2.360	0.6577
	Dif$^{1/1}$ - *Vago*$^{DM10/DM10}$	-0.7076	0.130	Inf	-5.459	**<0.0001**
	Dif$^{1/1}$ - *Egfr*$^{t1/t1}$	-0.7070	0.130	Inf	-5.454	**<0.0001**
	Rel$^{E20/20}$ - *Vago*$^{DM10/DM10}$	-0.4017	0.124	Inf	-3.240	**0.0431**
	Rel$^{E20/20}$ - *Egfr*$^{t1/t1}$	0.4011	0.124	Inf	3.235	**0.0438**
	Vago$^{DM10/DM10}$ - *Egfr*$^{t1/t1}$	-0.0006	0.124	Inf	-0.005	1.0000
All fly genotypes, all viral passages	5'UTR IRES - ORF1	-0.472	0.0512	Inf	-9.214	**<0.0001**
	5'UTR IRES - ORF2	-0.597	0.0512	Inf	-11.660	**<0.0001**
	ORF1 - ORF2	-0.125	0.0512	Inf	-2.450	0.0857
	3'UTR - ORF1	-1.348	0.0645	Inf	-20.915	**<0.0001**
	3'UTR - ORF2	-1.473	0.0645	Inf	-22.860	**<0.0001**
	3'UTR - 5'UTR IRES	-0.876	0.0645	Inf	-13.577	**<0.0001**
Full length DCV genome, P1	*w*^{1118} - *Dcr-2*$^{L811fsX/L811fsX}$	-0.6811	0.605	10	-1.126	1.0000
	w^{1118} - *Dcr-2*$^{R416X/R416X}$	-0.5391	0.605	10	-0.891	1.0000
	w^{1118} - *Ago-2*$^{414/41}$	0.0175	0.605	10	0.029	1.0000
	w^{1118} - *spz*$^{2/2}$	0.0840	0.605	10	0.139	1.0000
	w^{1118} - *Dif*$^{1/1}$	0.0457	0.605	10	0.076	1.0000
	w^{1118} - *Rel*$^{E20/20}$	0.3081	0.605	10	0.509	1.0000
	w^{1118} - *Vago*$^{DM10/DM10}$	-0.5342	0.605	10	-0.883	1.0000
	w^{1118} - *Egfr*$^{t1/t1}$	0.2863	0.605	10	0.473	1.0000
	w^{1118} - DCV stock R1	0.3363	0.605	10	0.556	1.0000
	w^{1118} - DCV stock R2	0.2992	0.605	10	0.495	1.0000
	Dcr-2$^{L811fsX/L811fsX}$ - *Dcr-2*$^{R416X/R416X}$	0.1420	0.605	10	0.235	1.0000
	Dcr-2$^{L811fsX/L811fsX}$ - *Ago-2*$^{414/414}$	0.6986	0.605	10	1.155	1.0000
	Dcr-2$^{L811fsX/L811fsX}$ - *spz*$^{2/2}$	-0.7651	0.605	10	-1.265	1.0000
	Dcr-2$^{L811fsX/L811fsX}$ - *Dif*$^{1/1}$	-0.7268	0.605	10	-1.202	1.0000
	Dcr-2$^{L811fsX/L811fsX}$ - *Rel*$^{E20/20}$	-0.9892	0.605	10	-1.636	1.0000
	Dcr-2$^{L811fsX/L811fsX}$ - *Vago*$^{DM10/DM10}$	-0.1470	0.605	10	-0.243	1.0000
	Dcr-2$^{L811fsX/L811fsX}$ - *Egfr*$^{t1/t1}$	-0.9674	0.605	10	-1.600	1.0000
	Dcr-2$^{L811fsX/L811fsX}$ - DCV stock R1	-1.0174	0.605	10	-1.682	1.0000
	Dcr-2$^{L811fsX/L811fsX}$ - DCV stock R2	-0.9803	0.605	10	-1.621	1.0000
	Dcr-2$^{R416X/R416X}$ - *Ago-2*$^{414/414}$	0.5566	0.605	10	0.920	1.0000
	Dcr-2$^{R416X/R416X}$ - *spz*$^{2/2}$	-0.6230	0.605	10	-1.030	1.0000
	Dcr-2$^{R416X/R416X}$ - *Dif*$^{1/1}$	-0.5848	0.605	10	-0.967	1.0000
	Dcr-2$^{R416X/R416X}$ - *Rel*$^{E20/20}$	-0.8472	0.605	10	-1.401	1.0000
	Dcr-2$^{R416X/R416X}$ - *Vago*$^{DM10/DM10}$	-0.0049	0.605	10	-0.008	1.0000
	Dcr-2$^{R416X/R416X}$ - *Egfr*$^{t1/t1}$	-0.8253	0.605	10	-1.365	1.0000
	Dcr-2$^{R416X/R416X}$ - DCV stock R1	-0.8754	0.605	10	-1.447	1.0000
	Dcr-2$^{R416X/R416X}$ - DCV stock R2	-0.8383	0.605	10	-1.386	1.0000
	Ago-2$^{414/414}$ - *spz*$^{2/2}$	-0.0665	0.605	10	-0.110	1.0000
	Ago-2$^{414/414}$ - *Dif*$^{1/1}$	-0.0282	0.605	10	-0.047	1.0000

	Ago-2$^{414/414}$ - *Rel$^{E20/20}$*	-0.2906	0.605	10	-0.481	1.0000
	Ago-2$^{414/414}$ - *Vago$^{DM10/DM10}$*	0.5517	0.605	10	0.912	1.0000
	Ago-2$^{414/414}$ - *Egfr$^{t1/t1}$*	-0.2688	0.605	10	-0.444	1.0000
	Ago-2$^{414/414}$ - DCV stock R1	-0.3188	0.605	10	-0.527	1.0000
	Ago-2$^{414/414}$ - DCV stock R2	-0.2817	0.605	10	-0.466	1.0000
	spz$^{2/2}$ - *Dif$^{1/1}$*	-0.0383	0.605	10	-0.063	1.0000
	spz$^{2/2}$ - *Rel$^{E20/20}$*	0.2242	0.605	10	0.371	1.0000
	spz$^{2/2}$ - *Vago$^{DM10/DM10}$*	0.6181	0.605	10	1.022	1.0000
	spz$^{2/2}$ - *Egfr$^{t1/t1}$*	0.2023	0.605	10	0.335	1.0000
	spz$^{2/2}$ - DCV stock R1	0.2523	0.605	10	0.417	1.0000
	spz$^{2/2}$ - DCV stock R2	0.2152	0.605	10	0.356	1.0000
	Dif$^{1/1}$ - *Rel$^{E20/20}$*	-0.2624	0.605	10	-0.434	1.0000
	Dif$^{1/1}$ - *Vago$^{DM10/DM10}$*	0.5799	0.605	10	0.959	1.0000
	Dif$^{1/1}$ - *Egfr$^{t1/t1}$*	-0.2406	0.605	10	-0.398	1.0000
	Dif$^{1/1}$ - DCV stock R1	-0.2906	0.605	10	-0.481	1.0000
	Dif$^{1/1}$ - DCV stock R2	-0.2535	0.605	10	-0.419	1.0000
	Rel$^{E20/20}$ - *Vago$^{DM10/DM10}$*	0.8423	0.605	10	1.393	1.0000
	Rel$^{E20/20}$ - *Egfr$^{t1/t1}$*	-0.0219	0.605	10	-0.036	1.0000
	Rel$^{E20/20}$ - DCV stock R1	0.0282	0.605	10	0.047	1.0000
	Rel$^{E20/20}$ - DCV stock R2	-0.0089	0.605	10	-0.015	1.0000
	Vago$^{DM10/DM10}$ - *Egfr$^{t1/t1}$*	0.8204	0.605	10	1.357	1.0000
	Vago$^{DM10/DM10}$ - DCV Stock R1	0.8705	0.605	10	1.439	1.0000
	Vago$^{DM10/DM10}$ - DCV stock R2	0.8333	0.605	10	1.378	1.0000
	Egfr$^{t1/t1}$ - DCV stock R1	-0.0500	0.605	10	-0.083	1.0000
	Egfr$^{t1/t1}$ - DCV stock R2	-0.0129	0.605	10	-0.021	1.0000
	DCV stock R1 - DCV stock R2	0.0371	0.605	10	0.061	1.0000
Full length DCV genome, P5	*w^{1118}* - *Dcr-2$^{L811fsX/L811fsX}$*	0.6418	0.29	10	2.217	1.0000
	w^{1118} - *Dcr-2$^{R416X/R416X}$*	0.5894	0.29	10	2.036	1.0000
	w^{1118} - *Ago-2$^{414/41}$*	0.5614	0.29	10	1.939	1.0000
	w^{1118} - *spz$^{2/2}$*	0.5482	0.29	10	1.894	1.0000
	w^{1118} - *Dif$^{1/1}$*	0.4524	0.29	10	1.563	1.0000
	w^{1118} - *Rel$^{E20/20}$*	0.2449	0.29	10	0.846	1.0000
	w^{1118} - *Vago$^{DM10/DM10}$*	1.0051	0.29	10	3.471	0.3303
	w^{1118} - *Egfr$^{t1/t1}$*	0.7169	0.29	10	2.476	1.0000
	w^{1118} - DCV stock R1	1.4714	0.29	10	5.082	**0.0262**
	w^{1118} - DCV stock R2	1.4343	0.29	10	4.954	**0.0316**
	Dcr-2$^{L811fsX/L811fsX}$ - *Dcr-2$^{R416X/R416X}$*	-0.0524	0.29	10	-0.181	1.0000
	Dcr-2$^{L811fsX/L811fsX}$ - *Ago-2$^{414/414}$*	-0.0804	0.29	10	-0.278	1.0000
	Dcr-2$^{L811fsX/L811fsX}$ - *spz$^{2/2}$*	0.0936	0.29	10	0.323	1.0000
	Dcr-2$^{L811fsX/L811fsX}$ - *Dif$^{1/1}$*	0.1894	0.29	10	0.654	1.0000

Dcr-2$^{L811fsX/L811fsX}$ - *Rel*$^{E20/20}$	0.3969	0.29	10	1.371	1.0000
Dcr-2$^{L811fsX/L811fsX}$ - *Vago*$^{DM10/DM10}$	-0.3633	0.29	10	-1.255	1.0000
Dcr-2$^{L811fsX/L811fsX}$ - *Egfr*$^{t1/t1}$	-0.0751	0.29	10	-0.259	1.0000
Dcr-2$^{L811fsX/L811fsX}$ - DCV stock R1	-0.8296	0.29	10	-2.865	0.9240
Dcr-2$^{L811fsX/L811fsX}$ - DCV stock R2	-0.7925	0.29	10	-2.737	1.0000
Dcr-2$^{R416X/R416X}$ - *Ago-2*$^{414/414}$	-0.0280	0.29	10	-0.097	1.0000
Dcr-2$^{R416X/R416X}$ - *spz*$^{2/2}$	0.0411	0.29	10	0.142	1.0000
Dcr-2$^{R416X/R416X}$ - *Dif*$^{1/1}$	0.1369	0.29	10	0.473	1.0000
Dcr-2$^{R416X/R416X}$ - *Rel*$^{E20/20}$	0.3444	0.29	10	1.190	1.0000
Dcr-2$^{R416X/R416X}$ - *Vago*$^{DM10/DM10}$	-0.4157	0.29	10	-1.436	1.0000
Dcr-2$^{R416X/R416X}$ - *Egfr*$^{t1/t1}$	-0.1275	0.29	10	-0.441	1.0000
Dcr-2$^{R416X/R416X}$ - DCV stock R1	-0.8821	0.29	10	-3.047	0.6778
Dcr-2$^{R416X/R416X}$ - DCV stock R2	-0.8449	0.29	10	-2.918	0.8440
Ago-2$^{414/414}$ - *spz*$^{2/2}$	0.0132	0.29	10	0.045	1.0000
Ago-2$^{414/414}$ - *Dif*$^{1/1}$	0.1090	0.29	10	0.376	1.0000
Ago-2$^{414/414}$ - *Rel*$^{E20/20}$	0.3165	0.29	10	1.093	1.0000
Ago-2$^{414/414}$ - *Vago*$^{DM10/DM10}$	-0.4437	0.29	10	-1.532	1.0000
Ago-2$^{414/414}$ - *Egfr*$^{t1/t1}$	-0.1555	0.29	10	-0.537	1.0000
Ago-2$^{414/414}$ - DCV stock R1	-0.9100	0.29	10	-3.143	0.5750
Ago-2$^{414/414}$ - DCV stock R2	-0.8729	0.29	10	-3.015	0.7155
spz$^{2/2}$ - *Dif*$^{1/1}$	-0.0958	0.29	10	-0.331	1.0000
spz$^{2/2}$ - *Rel*$^{E20/20}$	-0.3033	0.29	10	-1.048	1.0000
spz$^{2/2}$ - *Vago*$^{DM10/DM10}$	-0.4569	0.29	10	-1.578	1.0000
spz$^{2/2}$ - *Egfr*$^{t1/t1}$	0.1687	0.29	10	0.583	1.0000
spz$^{2/2}$ - DCV stock R1	0.9232	0.29	10	3.189	0.5323
spz$^{2/2}$ - DCV stock R2	0.8861	0.29	10	3.060	0.6621
Dif$^{1/1}$ - *Rel*$^{E20/20}$	0.2075	0.29	10	0.717	1.0000
Dif$^{1/1}$ - *Vago*$^{DM10/DM10}$	-0.5527	0.29	10	-1.909	1.0000
Dif$^{1/1}$ - *Egfr*$^{t1/t1}$	-0.2645	0.29	10	-0.914	1.0000
Dif$^{1/1}$ - DCV stock R1	-1.0190	0.29	10	-3.520	0.3049
Dif$^{1/1}$ - DCV stock R2	-0.9819	0.29	10	-3.391	0.3779
Rel$^{E20/20}$ - *Vago*$^{DM10/DM10}$	-0.7602	0.29	10	-2.626	1.0000
Rel$^{E20/20}$ - *Egfr*$^{t1/t1}$	0.4720	0.29	10	1.630	1.0000
Rel$^{E20/20}$ - DCV stock R1	1.2265	0.29	10	4.236	0.0950
Rel$^{E20/20}$ - DCV stock R2	1.1894	0.29	10	4.108	0.1165
Vago$^{DM10/DM10}$ - *Egfr*$^{t1/t1}$	-0.2882	0.29	10	-0.995	1.0000
Vago$^{DM10/DM10}$ - DCV Stock R1	0.4663	0.29	10	1.611	1.0000
Vago$^{DM10/DM10}$ - DCV stock R2	0.4292	0.29	10	1.482	1.0000
Egfr$^{t1/t1}$ - DCV stock R1	-0.7545	0.29	10	-2.606	1.0000
Egfr$^{t1/t1}$ - DCV stock R2	-0.7174	0.29	10	-2.478	1.0000
DCV stock R1 - DCV stock R2	0.0371	0.29	10	0.128	1.0000

Full length DCV genome, P10	*w*^{1118} - *Dcr-2*$^{L811fsX/L811fsX}$	0.1642	0.246	10	0.668	1.0000
	w^{1118} - *Dcr-2*$^{R416X/R416X}$	0.4977	0.246	10	2.026	1.0000
	w^{1118} - *Ago-2*$^{414/41}$	0.4988	0.246	10	2.031	1.0000
	w^{1118} - *spz*$^{2/2}$	-0.0775	0.246	10	-0.316	1.0000
	w^{1118} - *Dif*$^{1/1}$	-0.3342	0.246	10	-1.361	1.0000
	w^{1118} - *Rel*$^{E20/20}$	0.0590	0.246	10	0.240	1.0000
	w^{1118} - *Vago*$^{DM10/DM10}$	0.4039	0.246	10	1.644	1.0000
	w^{1118} - *Egfr*$^{t1/t1}$	0.4290	0.246	10	1.746	1.0000
	w^{1118} - DCV stock R1	1.2133	0.246	10	4.940	**0.0323**
	w^{1118} - DCV stock R2	1.1762	0.246	10	4.788	**0.0405**
	Dcr-2$^{L811fsX/L811fsX}$ - *Dcr-2*$^{R416X/R416X}$	0.3335	0.246	10	1.358	1.0000
	Dcr-2$^{L811fsX/L811fsX}$ - *Ago-2*$^{414/414}$	0.3346	0.246	10	1.362	1.0000
	Dcr-2$^{L811fsX/L811fsX}$ - *spz*$^{2/2}$	0.2417	0.246	10	0.984	1.0000
	Dcr-2$^{L811fsX/L811fsX}$ - *Dif*$^{1/1}$	0.4984	0.246	10	2.029	1.0000
	Dcr-2$^{L811fsX/L811fsX}$ - *Rel*$^{E20/20}$	0.1052	0.246	10	0.428	1.0000
	Dcr-2$^{L811fsX/L811fsX}$ - *Vago*$^{DM10/DM10}$	-0.2397	0.246	10	-0.976	1.0000
	Dcr-2$^{L811fsX/L811fsX}$ - *Egfr*$^{t1/t1}$	-0.2648	0.246	10	-1.078	1.0000
	Dcr-2$^{L811fsX/L811fsX}$ - DCV stock R1	-1.0491	0.246	10	-4.271	0.0899
	Dcr-2$^{L811fsX/L811fsX}$ - DCV stock R2	-1.0120	0.246	10	-4.120	0.1142
	Dcr-2$^{R416X/R416X}$ - *Ago-2*$^{414/414}$	0.0011	0.246	10	0.004	1.0000
	Dcr-2$^{R416X/R416X}$ - *spz*$^{2/2}$	0.5752	0.246	10	2.342	1.0000
	Dcr-2$^{R416X/R416X}$ - *Dif*$^{1/1}$	0.8319	0.246	10	3.387	0.3806
	Dcr-2$^{R416X/R416X}$ - *Rel*$^{E20/20}$	0.4387	0.246	10	1.786	1.0000
	Dcr-2$^{R416X/R416X}$ - *Vago*$^{DM10/DM10}$	0.0939	0.246	10	0.382	1.0000
	Dcr-2$^{R416X/R416X}$ - *Egfr*$^{t1/t1}$	0.0688	0.246	10	0.280	1.0000
	Dcr-2$^{R416X/R416X}$ - DCV stock R1	-0.7156	0.246	10	-2.913	0.8512
	Dcr-2$^{R416X/R416X}$ - DCV stock R2	-0.6785	0.246	10	-2.762	1.0000
	Ago-2$^{414/414}$ - *spz*$^{2/2}$	0.5763	0.246	10	2.346	1.0000
	Ago-2$^{414/414}$ - *Dif*$^{1/1}$	0.8330	0.246	10	3.391	0.3778
	Ago-2$^{414/414}$ - *Rel*$^{E20/20}$	0.4398	0.246	10	1.791	1.0000
	Ago-2$^{414/414}$ - *Vago*$^{DM10/DM10}$	0.0950	0.246	10	0.387	1.0000
	Ago-2$^{414/414}$ - *Egfr*$^{t1/t1}$	0.0699	0.246	10	0.284	1.0000
	Ago-2$^{414/414}$ - DCV stock R1	-0.7145	0.246	10	-2.909	0.8578
	Ago-2$^{414/414}$ - DCV stock R2	-0.6774	0.246	10	-2.758	1.0000
	spz$^{2/2}$ - *Dif*$^{1/1}$	-0.2567	0.246	10	-1.045	1.0000
	spz$^{2/2}$ - *Rel*$^{E20/20}$	0.1365	0.246	10	0.556	1.0000
	spz$^{2/2}$ - *Vago*$^{DM10/DM10}$	-0.4814	0.246	10	-1.960	1.0000
	spz$^{2/2}$ - *Egfr*$^{t1/t1}$	0.5065	0.246	10	2.062	1.0000
	spz$^{2/2}$ - DCV stock R1	1.2908	0.246	10	5.255	**0.0204**
	spz$^{2/2}$ - DCV stock R2	1.2537	0.246	10	5.104	**0.0254**
	Dif$^{1/1}$ - *Rel*$^{E20/20}$	-0.3932	0.246	10	-1.601	1.0000

Dif$^{1/1}$ - *Vago*$^{DM10/DM10}$	-0.7381	0.246	10	-3.005	0.7278
Dif$^{1/1}$ - *Egfr*$^{t1/t1}$	-0.7632	0.246	10	-3.107	0.6114
Dif$^{1/1}$ - DCV stock R1	-1.5475	0.246	10	-6.300	**0.0049**
Dif$^{1/1}$ - DCV stock R2	-1.5104	0.246	10	-6.149	**0.0060**
Rel$^{E20/20}$ - *Vago*$^{DM10/DM10}$	-0.3449	0.246	10	-1.404	1.0000
Rel$^{E20/20}$ - *Egfr*$^{t1/t1}$	0.3700	0.246	10	1.506	1.0000
Rel$^{E20/20}$ - DCV stock R1	1.1543	0.246	10	4.699	**0.0463**
Rel$^{E20/20}$ - DCV stock R2	1.1172	0.246	10	4.548	0.0584
Vago$^{DM10/DM10}$ - *Egfr*$^{t1/t1}$	0.0251	0.246	10	0.102	1.0000
Vago$^{DM10/DM10}$ - DCV Stock R1	0.8094	0.246	10	3.295	0.4441
Vago$^{DM10/DM10}$ - DCV stock R2	0.7723	0.246	10	3.144	0.5739
Egfr$^{t1/t1}$ - DCV stock R1	-0.7843	0.246	10	-3.193	0.5281
Egfr$^{t1/t1}$ - DCV stock R2	-0.7472	0.246	10	-3.042	0.6830
DCV stock R1 - DCV stock R2	0.0371	0.246	10	0.151	1.0000

Supplementary Table 2. Statistical analysis of the fly survival curves from Figure 5a. The table shows the number of flies used in the experiments, the median survival of the flies in each experimental setting and the *p* values of pairwise comparisons of the survival curves determined by Log-rank (Mantel–Cox) tests. These analyses were performed using GraphPad Prism 8.4.3.

Viral Passage 1 – Biological replicate 1

Viral stock Origin	Nr. of flies	Median survival	Viral stock Origin										
			Mock	**S2 DCV stock**	**DCV stock**	***w*^{1118}**	***Dcr-2*$^{L811fsX/L811fsX}$**	***Dcr-2*$^{R416X/R416X}$**	***Ago-2*$^{414/414}$**	***spz*$^{2/2}$**	***Dif*$^{1/1}$**	***Rel*$^{E20/20}$**	***Vago*$^{DM10/DM10}$**
Mock	235	Und.											
S2 DCV stock	235	5	<0,0001										
DCV stock	231	6	<0,0001 ****	<0,0001 ****									
***w*^{1118}**	119	5	<0,0001 ****	0,1152 ns	<0,0001 ****								
***Dcr-2*$^{L811fsX/L811fsX}$**	120	4	<0,0001 ****	<0,0001 ****	<0,0001 ****	<0,0001 ****							
***Dcr-2*$^{R416X/R416X}$**	118	5	<0,0001 ****	0,3054 ns	<0,0001 ****	0,6783 ns	<0,0001 ****						
***Ago-2*$^{414/414}$**	120	4	<0,0001 ****	<0,0001 ****	<0,0001 ****	<0,0001 ****	0,1412 ns	<0,0001 ****					
***spz*$^{2/2}$**	119	5	<0,0001 ****	0,2037 ns	<0,0001 ****	0,0007 ***	<0,0001 ****	0,0061 **	<0,0001 ****				
***Dif*$^{1/1}$**	117	5	<0,0001 ****	0,0888 ns	<0,0001 ****	0,8372 ns	<0,0001 ****	0,7587 ns	<0,0001 ****	0,0004 ***			
***Rel*$^{E20/20}$**	118	5	<0,0001 ****	<0,0001 ****	<0,0001 ****	0,0222 *	<0,0001 ****	0,0024 **	0,0007 ***	<0,0001 ****	0,0044 **		
***Vago*$^{DM10/DM10}$**	120	5	<0,0001 ****	0,0038 **	<0,0001 ****	0,3019 ns	<0,0001 ****	0,1366 ns	0,0004 ***	<0,0001 ****	0,1696 ns	0,3443 ns	
***Egfr*$^{t1/t1}$**	119	6	<0,0001 ****	<0,0001 ****	0,0002 ***	<0,0001 ****	<0,0001 ****	<0,0001 ****	<0,0001 ****	0,0038 **	<0,0001 ****	<0,0001 ****	<0,0001 ****

Viral Passage 10 – Biological replicate 1

Viral stock Origin	Nr. of flies	Median survival	Viral stock Origin										
			Mock	**S2 DCV stock**	**DCV stock**	***w*^{1118}**	***Dcr-2*$^{L811fsX/L811fsX}$**	***Dcr-2*$^{R416X/R416X}$**	***Ago-2*$^{414/414}$**	***spz*$^{2/2}$**	***Dif*$^{1/1}$**	***Rel*$^{E20/20}$**	***Vago*$^{DM10/DM10}$**
Mock	235	Und.											

S2 DCV stock	235	5	<0,0001 ****											
DCV stock	231	6	<0,0001 ****	<0,0001 ****										
***w*^{1118}**	116	6	<0,0001 ****	0,3626 ns	<0,0001 ****									
***Dcr-2*$^{L811fsX/L811fsX}$**	114	6	<0,0001 ****	<0,0001 ****	0,0655 *ns*	<0,0001 ****								
***Dcr-2*$^{R416X/R416X}$**	106	6	<0,0001 ****	0,0008 ***	<0,0001 ****	0,0228 *	0,0029 **							
***Ago-2*$^{414/414}$**	115	6	<0,0001 ****	<0,0001 ****	0,5588 ns	<0,0001 ****	0,1497 ns	0,0003 ***						
***spz*$^{2/2}$**	118	5	<0,0001 ****	0,353 ns	<0,0001 ****	0,6788 ns	<0,0001 ****	0,004 **	<0,0001 ****					
***Dif*$^{1/1}$**	117	6	<0,0001 ****	0,0063 **	<0,0001 ****	0,1699 ns	<0,0001 ****	0,2717 ns	<0,0001 ****	0,0416 *				
***Rel*$^{E20/20}$**	110	6	<0,0001 ****	<0,0001 ****	0,0020 **	0,0027 **	0,2122 ns	0,2453 ns	0,0185 *	0,0014 **	0,0493 *			
***Vago*$^{DM10/DM10}$**	108	5	<0,0001 ****	0,0126 *	<0,0001 ****	0,147 ns	0,0003 ***	0,428 ns	<0,0001 ****	0,074 ns	0,9034 ns	0,066 ns		
***Egfr*$^{t1/t1}$**	115	6	<0,0001 ****	<0,0001 ****	0,8472 ns	<0,0001 ****	0,017 *	<0,0001 ****	0,607 ns	<0,0001 ****	<0,0001 ****	0,0011 **	<0,0001 ****	

Viral Passage 1 – Biological replicate 2

Viral stock Origin	**Nr. of flies**	**Median survival**	**Viral stock Origin**										
			Mock	**S2 DCV stock**	**DCV stock**	***w*^{1118}**	***Dcr-2*$^{L811fsX/L811fsX}$**	***Dcr-2*$^{R416X/R416X}$**	***Ago-2*$^{414/414}$**	***spz*$^{2/2}$**	***Dif*$^{1/1}$**	***Rel*$^{E20/20}$**	***Vago*$^{DM10/DM10}$**
Mock	235	Und.											
S2 DCV stock	225	5	<0,0001 ****										
DCV stock	233	6	<0,0001 ****	<0,0001 ****									
***w*^{1118}**	119	4	<0,0001 ****	<0,0001 ****	<0,0001 ****								
***Dcr-2*$^{L811fsX/L811fsX}$**	119	5	<0,0001 ****	0,0209 *	<0,0001 ****	0,0300 *							
***Dcr-2*$^{R416X/R416X}$**	119	5	<0,0001 ****	0,2219 ns	<0,0001 ****	<0,0001 ****	0,0012 **						
***Ago-2*$^{414/414}$**	118	4	<0,0001	<0,0001	<0,0001	0,3835	0,0025	<0,0001					

			****	****	****	ns	**	****					
***spz*$^{2/2}$**	119	5	<0,0001	0,2456	<0,0001	<0,0001	0,0011	0,9665	<0,0001				
			****	ns	****	****	**	ns	****				
***Dif*$^{1/1}$**	119	4	<0,0001	<0,0001	<0,0001	0,2122	0,3402	<0,0001	0,0329	<0,0001			
			****	****	****	ns	ns	****	*	****			
***Rel*$^{E20/20}$**	120	5	<0,0001	<0,0001	<0,0001	0,009	0,6047	0,0062	0,0005	0,005	0,1455		
			****	****	****	**	ns	**	***	**	ns		
***Vago*$^{DM10/DM10}$**	120	6	<0,0001	<0,0001	<0,0001	<0,0001	<0,0001	<0,0001	<0,0001	<0,0001	<0,0001	<0,0001	
			****	****	****	****	****	****	****	****	****	****	
***Egfr*$^{t1/t1}$**	115	5	<0,0001	0,1738	0,5815	<0,0001	0,0005	0,1995	<0,0001	0,1971	<0,0001	0,0016	0,0033
			****	ns	ns	****	***	ns	****	ns	****	**	**

Viral Passage 10 – Biological replicate 2

Viral stock Origin	**Nr. of flies**	**Median survival**	**Viral stock Origin**										
			Mock	**S2 DCV stock**	**DCV stock**	***w*^{1118}**	***Dcr-2*$^{L811fsX/L811fsX}$**	***Dcr-2*$^{R416X/R416X}$**	***Ago-2*$^{414/414}$**	***spz*$^{2/2}$**	***Dif*$^{1/1}$**	***Rel*$^{E20/20}$**	***Vago*$^{DM10/DM10}$**
Mock	235	Und.											
S2 DCV stock	225	5	<0,0001										
			****										
DCV stock	233	6	<0,0001	<0,0001									
			****	****									
***w*^{1118}**	104	5	<0,0001	0,0209	0,0083								
			****	*	**								
***Dcr-2*$^{L811fsX/L811fsX}$**	105	5	<0,0001	0,1381	0,0004	0,3873							
			****	ns	***	ns							
***Dcr-2*$^{R416X/R416X}$**	110	5	<0,0001	0,0011	0,0211	0,6294	0,1213						
			****	**	*	ns	ns						
***Ago-2*$^{414/414}$**	111	5	<0,0001	0,1376	0,0005	0,4395	0,9246	0,1763					
			****	ns	***	ns	ns	ns					
***spz*$^{2/2}$**	102	5	<0,0001	0,0003	0,2429	0,2615	0,0400	0,3852	0,0602				
			****	***	ns	ns	*	ns	ns				
***Dif*$^{1/1}$**	98	5	<0,0001	0,0979	0,0018	0,5727	0,698	0,3219	0,8399	0,1019			
			****	ns	**	ns	ns	ns	ns	ns			
***Rel*$^{E20/20}$**	100	5	<0,0001	0,0905	0,002	0,6142	0,7401	0,3066	0,7993	0,1219	0,9375		
			****	ns	**	ns	ns	ns	ns	ns	ns		
***Vago*$^{DM10/DM10}$**	94	5	<0,0001	0,0013	0,1121	0,3741	0,0779	0,5576	0,0992	0,8418	0,146	0,1781	
			****	**	ns	ns	ns	ns	ns	ns	ns	ns	
***Egfr*$^{t1/t1}$**	98	5	<0,0001	0,0297	0,0101	0,9411	0,4563	0,5765	0,5522	0,1878	0,7472	0,7471	0,3464
			****	*	*	ns	ns	ns	ns	ns	ns	ns	ns

```
library(Hmisc)
library(corrplot)
library(PerformanceAnalytics)
library(xlsx)
library(EvoFreq)
library(timescape)

setwd("~/Documents/Virus/SINV/calder")

# Read a file with t (passage) rows and l (locus) columns.  Cells
represent the number of copies

rawdatos = read.table("./Sudden.5/Sudden.5.txt", header = T)
datos = rawdatos

# Replace zero values by NA and compute logits

for (p in (1:nrow(datos)))
   {
    for (l in (2:ncol(datos)))
      {
       if (datos[p, l] == 0 | datos[p, l] == 1000)
          {
           datos[p, l] = NA
          }
       else
          {
           datos[p, l] = log(datos[p, l]/(1000 - datos[p, l]), base
= 10)
          }
      }
    }
fitness = array(NA, dim = ncol(datos) - 1)
errfitness = array(NA, dim = ncol(datos) - 1)
pvaluet = array(NA, dim = ncol(datos) - 1)
ncases = array(NA, dim = ncol(datos) - 1)

# Linear regressions.  Save fitness (10^slope), its error and
associated P values

for (locus in 2:ncol(datos))
  {
   reglogit = summary(lm(datos[, locus] ~ datos[, 1],
na.omit(datos)))
   fitness[locus] = 10^reglogit$coefficients[2]
   errfitness[locus] = fitness[locus]*reglogit$coefficients[4]
   pvaluet[locus] = reglogit$coefficients[8]
   ncases[locus] = length(na.omit(datos[, locus]))
  }
FDRvalue = p.adjust(pvaluet, method = "BH", n = length(pvaluet))
Result = data.frame(Locus = colnames(datos[2:ncol(datos)] - 1),
Fitness = c(fitness[2:ncol(datos)]), SEM_fitness =
c(errfitness[2:ncol(datos)]), n_cases = c(ncases[2:ncol(datos)]), P
= c(pvaluet[2:ncol(datos)]), FDR = c(FDRvalue[2:ncol(datos)]))
```

```
write.csv(Result, "./Sudden.5/Sudden.5.csv", row.names = F)

#
# Compute pairwise correlations to identify potential haplotypes
#

# +++++++++++++++++++++++++++
# flattenCorrMatrix
# +++++++++++++++++++++++++++
# cormat : matrix of the correlation coefficients
# pmat : matrix of the correlation p-values

flattenCorrMatrix <- function(cormat, pmat)
{
  ut <- upper.tri(cormat)
  data.frame(row = rownames(cormat)[row(cormat)[ut]], column =
rownames(cormat)[col(cormat)[ut]], cor = (cormat)[ut], p = pmat[ut])
}

datos_short = read.table("./Sudden.5/Sudden.5.txt", header = T)
corrdyn = rcorr(as.matrix(datos_short[, 2:ncol(datos_short)]), type
= c("pearson"))
Rescorr = flattenCorrMatrix(corrdyn$r, corrdyn$P)
write.csv(Rescorr, "./Sudden.5/Sudden.5corr.csv", row.names = F)
# corrplot(corrdyn$r, type = "upper", order = "hclust", tl.col =
"black", tl.srt = 45)
color = colorRampPalette(c("blue", "white", "red")) (20)
heatmap(x = corrdyn$r, col = color, symm = T)

#
# Prepare data to run CALDER and run EvoFreq or Timescape using
CALDER outputs
#

input = rawdatos
vecnames = array(NA, dim = ncol(input))
vecnames = c(colnames(input))
readycalder = matrix(NA, nrow = nrow(input), ncol = 2*ncol(input) -
1)
readynames = array(NA, dim = 2*ncol(input) - 1)
readynames[1] = "\t"
for (pase in 1:nrow(input))
   {
    readycalder[pase, 1] = input[pase, 1]
    for (locus in 2:ncol(input))
      {
       if(!is.na(errfitness[locus]) | !is.nan(errfitness[locus]))
          {
           readycalder[pase, 2*locus - 2] = 1000 - input[pase,
locus]
           readynames[2*locus - 2] = vecnames[locus]
           readycalder[pase, 2*locus - 1] = input[pase, locus]
           readynames[2*locus - 1] = vecnames[locus]
          }
```

```
      }
   }
write.table(rbind(readynames, readycalder), "./Sudden.5/
Sudden.5.input", sep ="\t", row.names = F, col.names = F)

#
# Running EvoFreq
#

long_to_wide_size_df = long_to_wide_freq_ready
theFile = "./Sudden.5/Sudden_tree1.dot"
theSoln = "./Sudden.5/Sudden_soln1.csv"
calder.data = parse_calder(theSoln, theFile)

clones <- as.character(calder.data$clones)
parents <- as.character(calder.data$parents)
size_df <- calder.data$wide_size_df
size_df <- size_df[order(as.numeric(colnames(size_df)))]
clone_dynamics_df <- get_evofreq(size_df, clones, parents,
clone_cmap = "jet", threshold = 0, fill_gaps_in_size = T)
plot_evofreq(clone_dynamics_df)


#
# Running Timescape
#

prev = read.table("./Gradual.101/Gradual.101_prev.txt", header = T)
edges = read.table("./Gradual.101/Gradual.101_edges.txt", header =
T)
timescape(clonal_prev = prev, tree_edges = edges, xaxis_title =
"Passage", yaxis_title = "Mutation abundance", phylogeny_title = "")
```